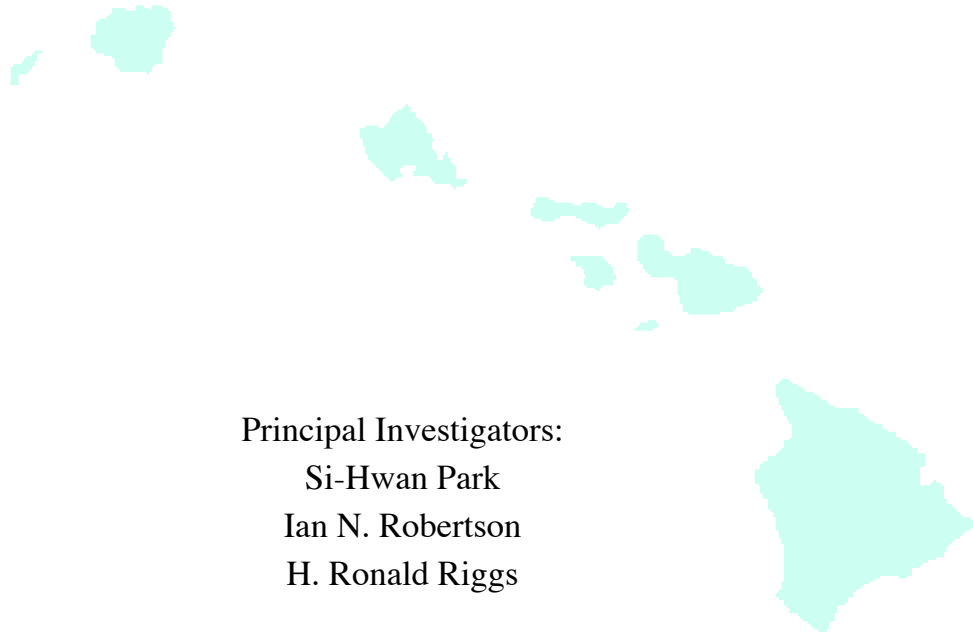


A Primer for FRP Strengthening of Structurally Deficient Bridges



Principal Investigators:

Si-Hwan Park

Ian N. Robertson

H. Ronald Riggs



Prepared in Cooperation with:

State of Hawaii, Department of Transportation, Highways Division

and

U.S. Department of Transportation, Federal Highway Administration

**UNIVERSITY OF HAWAII
COLLEGE OF ENGINEERING**

DEPARTMENT OF CIVIL AND ENVIRONMENTAL ENGINEERING

Research Report UHM/CE/02-03

September 2002

Technical Report Documentation Page

1. Report No. HWY-L-2001-01		2. Government Accession No		3. Recipient's Catalog No	
4. Title and Subtitle A Primer for FRP Strengthening of Structurally Deficient Bridges			5. Report Date September 20, 2002		
			6. Performing Organization Code		
7. Authors S.H. Park, I.N. Robertson, H.R. Riggs			8. Performing Organization Report No.		
9. Performing Organization Name and Address Department of Civil and Environmental Engineering University of Hawaii at Manoa 2540 Dole St. Holmes Hall 383 Honolulu, HI 96822			10. Work Unit No. (TRAIS)		
			11. Contract or Grant No. 47770		
12. Sponsoring Agency Name and Address Hawaii Department of Transportation Highways Division 869 Punchbowl St. Honolulu, HI 96813			13. Type of Report and Period Covered Final – Phase 1 5/01 – 9/02		
			14. Sponsoring Agency Code		
15. Supplementary Notes Prepared in cooperation with the U.S. Department of Transportation, Federal Highway Administration					
16. Abstract <p>Although fiber-reinforced polymers (FRP) have been used widely in the aerospace and automobile industries, its use in bridges and buildings is relatively new. Engineers and contractors in this area are not as comfortable designing with FRP as with the familiar materials of concrete, steel, and wood. In addition, the material itself does not have as long a track record in these applications. Nevertheless, the advantages of FRP for specific applications result in it being used more and more frequently for structural engineering applications, especially for strengthening and retrofitting existing structures made of reinforced concrete or masonry.</p> <p>One area in which FRP is being used more frequently is the strengthening of structurally deficient concrete bridges. Incentives for the use of FRP over traditional materials include the material's high stiffness-to-weight and strength-to-weight ratios, corrosion resistance, and constructability. Disincentives include unfamiliarity by engineers, cost, proprietary nature of the material, and lack of experienced construction personnel.</p> <p>The objective of this report is to provide the Hawaii Department of Transportation with a 'primer' for the use of FRP in strengthening structurally deficient concrete bridges. Its aim is to increase the engineer's familiarity with the products, and thereby contribute to the consideration of FRP for specific projects based on technical merit. It represents a first reference that engineers can use for a concise description of FRP, recent relevant applications, overview of the materials, and basic how-to design procedures and guidelines, including possible design solutions for common situations. Because FRP is a relatively new material with a relatively short track record in the area of bridge strengthening, field instrumentation, testing, and monitoring of the immediate and long-term behavior of FRP strengthened bridges are also discussed.</p> <p>This report draws heavily on other published reports and papers. It is not meant as a complete reference, but rather it directs the reader to more comprehensive documents for specific issues.</p>					
17. Key Words Fiber reinforced polymer (FRP) Structurally deficient bridges			18. Distribution Statement No restriction. This document is available to the public through the National Technical Information Service 5285 Port Royal Road, Springfield VA 22161		
19. Security Classif.(of this report) Unclassified		20. Security Classif. (of this page) Unclassified		21. No. of Pages 76	22. Price

A Primer for FRP Strengthening of Structurally Deficient Bridges

Principal Investigators:

Si-Hwan Park

Ian N. Robertson

H. Ronald Riggs

Prepared in Cooperation with:

State of Hawaii, Department of Transportation, Highways Division

and

U.S. Department of Transportation, Federal Highway Administration

September 2002

Executive Summary

Although fiber-reinforced polymers (FRP) have been used widely in the aerospace and automobile industries, its use in bridges and buildings is relatively new. Engineers and contractors in this area are not as comfortable designing with FRP as with the familiar materials of concrete, steel, and wood. In addition, the material itself does not have as long a track record in these applications. Nevertheless, the advantages of FRP for specific applications result in it being used more and more frequently for structural engineering applications, especially for strengthening and retrofitting existing structures made of reinforced concrete or masonry.

One area in which FRP is being used more frequently is the strengthening of structurally deficient concrete bridges. Incentives for the use of FRP over traditional materials include the material's high stiffness-to-weight and strength-to-weight ratios, corrosion resistance, and constructability. Disincentives include unfamiliarity by engineers, cost, proprietary nature of the material, and lack of experienced construction personnel.

The objective of this report is to provide the Hawaii Department of Transportation with a 'primer' for the use of FRP in strengthening structurally deficient concrete bridges. Its aim is to increase the engineer's familiarity with the products, and thereby contribute to the consideration of FRP for specific projects based on technical merit. It represents a first reference that engineers can use for a concise description of FRP, recent relevant applications, overview of the materials, and basic how-to design procedures and guidelines, including possible design solutions for common situations. Because FRP is a relatively new material with a relatively short track record in the area of bridge strengthening, field instrumentation, testing, and monitoring of the immediate and long-term behavior of FRP strengthened bridges are also discussed.

This report draws heavily on other published reports and papers. It is not meant as a complete reference, but rather it directs the reader to more comprehensive documents for specific issues.

Acknowledgements

This report was produced under Hawaii Department of Transportation's Project No. HWY-L-2001-01, 'Use of Advanced Composites for Hawaii Bridges with Application to Renovation of Historic Bridges,' with the University of Hawaii at Manoa. Mr. Paul Santo, Bridge Design Section, HDOT, was the technical contact.

The authors gratefully acknowledge the support received under this project.

Disclaimer

The contents of this report reflect the views of the authors, who are responsible for the facts and accuracy of the data presented herein. The contents do not necessarily reflect the official views or policies of the State of Hawaii, Department of Transportation or the Federal Highway Administration. This report does not constitute a standard, specification, or regulation.

Table of Contents

Executive Summary	i
Acknowledgements	iii
Table of Contents	v
List of Figures	vii
1.0 Introduction	1
1.1 Overview	1
1.2 Objective and Scope	1
2.0 Recent Applications of FRP to Bridges	3
2.1 Overview	3
2.2 Ibach Bridge	3
2.3 Nossa Senhora da Guia Bridge	3
2.4 South Broadway Railroad Overpass	4
2.5 Boone County Bridges	4
2.6 Kings Stormwater Channel Bridge	4
2.7 Scheyler Heim Lift Bridge	5
2.8 I-5/Gilman Bridge	5
2.9 Dickey Creek Bridge	5
2.10 Ohio's C4I Bridge Decks	5
3.0 Evaluation of Existing Bridges	7
3.1 Overview	7
3.2 Sufficiency Rating	7
3.3 Load Rating	10
4.0 FRP Materials	13
4.1 Overview	13
4.2 Fibers	13
4.3 Resins	14
4.4 Methods of Application	14
4.4.1 Wet Lay-Up Systems	14
4.4.2 Prepreg Systems	15
4.4.3 Precured Systems	15
5.0 Design of FRP Reinforcement	17
5.1 Overview	17
5.2 Design Principles	17
5.3 Flexural Strengthening	18
5.3.1 General Assumptions	18
5.3.2 Ultimate Strength	19
5.3.3 Strain Compatibility	20
5.3.4 Internal Force Equilibrium	20
5.3.5 Design Example	21

5.4	Shear Strengthening	24
5.4.1	Wrapping Schemes	24
5.4.2	Ultimate Strength.....	25
5.4.3	Shear Strength by FRP Reinforcement.....	26
5.4.4	Design Example.....	29
5.5	Typical Bridge Applications	31
5.5.1	Poured-in-place T-beam Bridges.....	31
5.5.2	Precast AASHTO-Type Girder Bridges	34
5.5.3	Multi-cell Box Girder Bridges.....	36
6.0	Application Procedures.....	39
6.1	Overview	39
6.2	Specification Overview	39
6.3	Recommended Specification.....	40
7.0	Load Test	47
7.1	Overview	47
7.2	Load Test Parameters	47
7.3	Analytical Modeling.....	48
7.4	Instrumentation.....	49
7.4.1	General.....	49
7.4.2	Types of Instrumentation.....	50
7.4.3	Strain Measurements	50
7.4.4	Deflection Measurements	51
7.4.5	Ambient Weather Conditions	53
7.4.6	Data Collection	54
7.5	Load Application.....	54
7.5.1	Load Test Execution	56
7.5.2	Evaluation of Results.....	56
8.0	Summary.....	59
	List of References	61
	Appendix A.....	65
A.1	Strain Measurements	65
A.2	Deflection Measurements.....	74

List of Figures

Figure 5-1: Complete wrapping.....	25
Figure 5-2: Partial wrapping.....	25
Figure 5-3: Elevation of typical T-beam bridge	32
Figure 5-4: T-beam girders with level beam soffits	32
Figure 5-5: T-beam girders with sloped soffits	33
Figure 5-6: Typical flexural strengthening of T-beam bridge.....	33
Figure 5-7: Typical shear strengthening of T-beam bridge.....	34
Figure 5-8: Elevation of typical AASHTO-type girder bridge.....	34
Figure 5-9: AASHTO-type girders.....	35
Figure 5-10: Typical flexural strengthening of AASHTO-type girder bridge	35
Figure 5-11: Typical shear strengthening of AASHTO-type girder bridge	36
Figure 5-12: Typical multi-cell box girder bridge.....	37
Figure 5-13: Typical flexural strengthening of multi-cell box girder bridge	37
Figure 5-14: Typical shear strengthening of multi-cell box girder bridge	38
Figure 7-1: Load-test on the North Halawa Valley Viaduct	55
Figure A-1: Geokon VCE-4200 vibrating wire strain gage designed for concrete	65
Figure A-2: a) VWSG manual readout box and b) automated datalogger	66
Figure A-3: Electrical resistance gages epoxy bonded to steel reinforcement.....	68
Figure A-4: Electrical resistance gage spot-welded to steel section.....	68
Figure A-5: Electrical resistance gage epoxy bonded to surface of concrete.....	69
Figure A-6: Fiber optic strain sensor for concrete embedment	70
Figure A-7: Operation of microbending fiber optic sensor	71
Figure A-8: Fabry-Perot in-line strain sensor	72
Figure A-9: Fabry-Perot terminal strain sensor	72
Figure A-10: Creating Bragg Grating fiber optic sensor.....	73
Figure A-11: Multiplexed Bragg Grating fiber optic sensors.....	73
Figure A-12: Baseline deflection system using taut piano wire as reference.....	75
Figure A-13: Components of baseline system.....	75
Figure A-14: Tiltmeter attached to concrete girder web	76

1.0 Introduction

1.1 Overview

Fiber-reinforced polymers (FRP) have been used widely in the aerospace and automobile industries. As such, engineers and fabricators in those fields are experienced in its application, and the material has a reasonably long track record. However, its use in structural engineering applications, such as bridges and buildings, is relatively new. Engineers and contractors in this area are not as familiar with the material, and they are therefore not as comfortable designing with this material as with the familiar materials of concrete, steel, and wood. In addition, the material itself does not have as long a track record in these applications. Nevertheless, the advantages of FRP for specific applications result in it being used more and more frequently for structural engineering applications. To date, many of the uses have been in strengthening and retrofitting existing structures made of reinforced concrete or masonry. Some application of FRP has also been made to new construction where it is the primary structural material.

One area in which FRP is being used more and more is the strengthening of structurally deficient concrete bridges. As is widely known, a significant percentage of the bridges in the U.S. are deficient, and FRP is being used together with traditional materials and approaches for the repair and upgrading of these bridges. A major goal in many applications has been to increase the load rating of older bridges without adversely affecting bridge aesthetics.

Incentives for the use of FRP over traditional materials include the material's high stiffness-to-weight and strength-to-weight ratios, corrosion resistance, and constructability. Disincentives include unfamiliarity by engineers, cost, proprietary nature of the material, and lack of experienced construction personnel.

1.2 Objective and Scope

The objective of this report is to provide the Hawaii Department of Transportation with a 'primer' for the use of FRP in strengthening structurally deficient concrete bridges. Its aim is to increase the engineer's familiarity with the products, and as such, contribute to the consideration of FRP for specific projects based on technical merits alone. It

represents a first reference that engineers can use for a concise description of FRP, recent relevant applications, overview of the materials, and basic how-to design procedures and guidelines. It draws heavily on other published reports and papers. It is not meant as a complete reference, but rather it directs the reader to more comprehensive documents for specific issues.

Chapter 2 describes some recent applications of FRP, with special emphasis on bridge strengthening. Chapter 3 discusses the evaluation of the load rating of existing bridges and of bridge deficiencies. Chapter 4 provides an overview of the different materials and products used in FRP. Chapter 5 provides a how-to discussion related to the design of FRP bridge strengthening systems, describing possible design solutions for common problems and structural systems. Chapter 6 provides a Guideline Specification for application of FRP materials. Because it is a relatively new material with a relatively short track record in the area of bridge strengthening, Chapter 7 discusses field instrumentation and testing of bridges aimed at monitoring the immediate and long-term behavior of FRP strengthened bridges. More detailed information of some of the relevant instrumentation is provided in Appendix A. A summary of our findings is provided in Chapter 8.

2.0 Recent Applications of FRP to Bridges

2.1 Overview

The use of FRP in the rehabilitation and repair of bridges has increased dramatically in recent years. Although many early applications occurred in Europe and Japan, application in the U.S. increased substantially in the late 1990s. The most common application of FRP to bridges is to increase the load rating by increasing the flexural and shear capacity. Such applications typically involve bonding thin FRP fabric to the bottom and sides of structural load-bearing members. The most common types of fabric involve carbon and/or glass fibers. Both materials have their advantages, as will be discussed later. Because carbon is much stronger, it appears to be used extensively in recent strengthening projects even though it is more costly. Repair and other applications are illustrated by the following examples of FRP use. The objective of this chapter is to discuss briefly some interesting applications, to demonstrate some past uses of FRP, and to provide references in which more detailed information of these applications can be found.

2.2 Ibach Bridge

It appears that the first bridge strengthened with carbon FRP was the Ibach Bridge in Lucerne, Switzerland (Meier et al., 1992). The middle 39-meter span of the continuous box beam bridge was damaged. The span is 16 meters wide and has a middle longitudinal web. The damage resulted from the severing of a prestressing tendon in the outer web. The repair involved applying a 2 mm thick by 150 mm wide carbon FRP laminate. The repair was successful, and possibly contributed to subsequent use of carbon FRP for bridge repair.

2.3 Nossa Senhora da Guia Bridge

The Nossa Senhora da Guia Bridge at Ponte de Lima, Portugal was strengthened with carbon FRP. The reinforced concrete, double-box beam vehicle bridge consists of several 164-ft spans. A design flaw resulted in inadequate flexural reinforcing, which led to longitudinal cracking on the underside of the top slab. A pretensioning system was used to apply negative moment to the bridge to close the cracks. Then, thin strips of

unidirectional, pultruded carbon fiber/epoxy strips were applied to the bottom of the slab. The strips have a tensile strength of 348 ksi and an elastic modulus of 23,200 ksi. The pretensioning was maintained for several days while the epoxy cured. Additional details can be found in DesJardin (2001).

2.4 South Broadway Railroad Overpass

The 37-span, 4-lane South Broadway Railroad Overpass in Wichita, Kansas, built in 1937, is 784 ft long and 44 ft wide. Evaluated in 1998, it had a sufficiency rating of 4. During extensive rehabilitation, 10 pier beams were externally post-tensioned with carbon FRP leadline rods (Svaty et al., 2000).

2.5 Boone County Bridges

The load ratings of three similar bridges in Missouri were increased from 15-tons to HS-20 after flexural and shear strengthening with carbon FRP. The single span, simply-supported bridges were constructed with precast reinforced concrete channel sections. Carbon FRP strips were placed on the bottom of the stems for flexural strengthening, and they were wrapped around the stems for shear strengthening. The strips had a design strength of 550 ksi and a modulus of 33,000 ksi. See Alkhrdaji (2002) for more details.

2.6 Kings Stormwater Channel Bridge

The Kings Stormwater Channel Bridge in Salton Sea, CA, with 2 spans, a length of 66 ft and a width of 42.5 ft, entered service in 2001. The bridge consists of FRP deck and girders supported by a reinforced concrete pier. The deck system is made up of fiberglass panels, and the supporting girders are carbon fiber. This ‘experimental’ bridge carries northbound traffic, including heavy trucks, from Mexico to the U.S. The bridge girders are the University of California at San Diego’s Carbon Shell System (CSS), which consists of thin carbon fiber/epoxy tubulars filled with lightweight concrete. The deck panels are fiberglass from Martin Marietta Composites. The bridge is fully instrumented with strain gages and accelerometers, and is monitored remotely. Additional details can be found in DesJardin (2001).

2.7 Scheyler Heim Lift Bridge

The Scheyler Heim Lift Bridge in Long Beach, CA is 1,212 ft long with 4 lanes. The steel lift deck has been replaced several times. Caltrans is investigating replacing the deck with a carbon fiber deck to improve durability and reduce maintenance. Lab testing of the system was completed in 2001, and installation of test panels is scheduled for 2002. The intent is to monitor the test panels for 1 year prior to proceeding with a complete replacement. Additional details can be found in Hranac (2001).

2.8 I-5/Gilman Bridge

The University of California at San Diego (UCSD) is constructing a composite demonstration bridge between parts of its campus separated by I-5. The steel cable-stayed bridge will use UCSD's CSS, CFRP tubes filled with concrete, for support girders. The girders will support hollow FRP transverse girders. FRP deck panels will support the RC deck (CT, 2001a).

2.9 Dickey Creek Bridge

In October 2001, the 38-foot Dickey Creek Bridge on Route 601 in Sugar Grove, VA was officially opened. It uses FRP 36" x 18" composite beams and has an AASHTO HS-20 rating. Carbon fibers are used in the flanges for strength, but E-glass fibers are used in the web to make the beams more economical. Additional details can be found in Strongwell (2002).

2.10 Ohio's C4I Bridge Decks

Ohio has installed 10 composite bridge decks under the National Composites Center's Composites FOR Infrastructure (C4I) program (CT, 2002). An additional 5 composite decks are scheduled to be installed this year. The latest (and largest date) deck is three spans and over 7,000 ft². The deck is instrumented and will be monitored.

3.0 Evaluation of Existing Bridges

3.1 Overview

To develop an appropriate FRP strengthening strategy, the condition of the existing structure should first be evaluated to: 1) prioritize the candidate bridges which are structurally deficient; 2) determine the condition of each structural member and identify the members to be strengthened; and 3) determine the required extra capacity to be achieved and evaluate the feasibility of using FRP strengthening schemes. The use of FRP can enhance primarily the load-carrying capacity of the bridge thus positively affecting the sufficiency rating, which describes the overall capacity of the bridge. This chapter is concerned with a brief description of how sufficiency rating is determined and how it is affected by the load-carrying capacity.

3.2 Sufficiency Rating

The sufficiency rating is a numeric value (from 0% to 100%) that is indicative of the bridge sufficiency to remain in service. A sufficiency rating of 100% represents an entirely sufficient bridge while a rating of 0% represents a deficient bridge. The calculation of sufficiency rating was developed by the Federal Highway Administration, and is being used by HDOT. Here, the essential ingredients of determining bridge sufficiency rating are described. Details can be found in FHWA (1995).

Sufficiency rating factor S ($0\% \leq S \leq 100\%$) is calculated as

$$S = S_1 + S_2 + S_3 - S_4 \quad (3.1)$$

where

S_1 = Structural adequacy and safety (55% max.)

S_2 = Serviceability and functional obsolescence (30% max.)

S_3 = Essential for public use (15% max.)

S_4 = Special reductions (13% max.)

While S_1 , the dominant factor, is related to the structural condition of the bridge, the other factors, S_2 , S_3 and S_4 , do not depend on the load-carrying capacity. Therefore, determination of S_1 only will be discussed in what follows.

S_1 is computed as:

$$S_1 = 55 - (A + B) \quad (3.2)$$

In the above equation, A and B represent the reduction of the sufficiency rating due to structural adequacy and safety, and load-carrying capacity, respectively.

A is determined based on the condition ratings of the superstructure, substructure and culverts. Condition ratings are used to describe the existing, in-place bridge as compared to the as-built condition. Evaluation is for the materials related, physical condition of the deck, superstructure, and substructure components of the bridge. It provides an overall characterization of the general condition of the entire component being rated as opposed to the localized or nominally occurring instances of deterioration or disrepair. Condition rating is primarily based on visual inspection and the load-carrying capacity is not used in evaluating it. The general condition ratings are described in Table 3-1.

After the condition ratings of superstructure, substructure and culverts are obtained, only the lowest rating code is applied to determine A , Table 3-2. It is implied that a rating code greater than 5 implies $A = 0\%$ (no reduction).

B is based on the load-carrying capacity, and is calculated as:

$$B = (32.4 - IR)^{1.5} \times 0.3254, \quad 0\% \leq B \leq 55\%, \quad (3.3)$$

where IR is the inventory rating in tons, which can be determined based on the procedure described in the following section. Thus, inventory rating of 32.4 ton or greater would result in $B = 0\%$ (no reduction). The calculation of B clearly indicates how the sufficiency rating is affected by the load-carrying capacity, and how FRP-strengthening can contribute to increase the rating.

Table 3-1 Condition Rating Guide

Code	Description
N	Not Applicable
9	Excellent condition
8	Very good condition – No problem noted.
7	Good condition – Some minor problems.
6	Satisfactory condition – Structural elements show some minor deterioration.
5	Fair condition – All primary structural elements are sound but may have minor section loss, cracking, spalling or scour.
4	Poor condition – Advanced section loss, deterioration, spalling, or scour.
3	Serious condition – Loss of section, deterioration, spalling or scour have seriously affected primary structural components. Local failures are possible. Fatigue cracks in steel or shear cracks in concrete may be present.
2	Critical condition – Advanced deterioration of primary structural elements. Fatigue cracks in steel or shear cracks in concrete may be present or scour may have removed substructure support. Unless closely monitored it may be necessary to close the bridge until corrective action is taken.
1	Imminent failure condition – Major deterioration or section loss present in critical structural components or obvious vertical or horizontal movement affecting structure stability. Bridge is closed to traffic but corrective action may put back in light service.
0	Failed condition – Out of service. Beyond corrective action.

Table 3-2 Rating Codes

Rating Code	<i>A</i>
≤ 2	55%
= 3	40%
= 4	25%
= 5	10%

3.3 Load Rating

Bridge load rating calculations provide a basis for determining the safe load-carrying capacity of a bridge. AASHTO has released a set of guidelines for this purpose, where three methods for load rating are provided. The Allowable Stress (AS) method and the Load Factor (LF) method are described in *Manual for Condition Evaluation of Bridges* (2000), whereas the Load and Resistance Factor (LRF) method can be found in *Guide Specification for Strength Evaluation of Existing Steel and Concrete Bridges* (1989). Because HDOT uses the Load Factor method, more emphasis will be placed on this method in describing the load-rating procedures, and the *Manual* should be referred to for more details.

The rating of a bridge member in tons, RT , is calculated as:

$$RT=(RF)W \quad (3.4)$$

where RF is the rating factor for the live-load carrying capacity and W is the weight (in tons) of the rating vehicle used to determine the live load effect. The rating factor is determined by the following equation:

$$RF = \frac{C - A_1D}{A_2L(1 + I)} \quad (3.5)$$

where C = the nominal capacity of the member, D = the dead load effect on the member, L = the live load effect on the member, I = the impact factor to be used with the live load effect, A_1 = dead load factor, and A_2 = live load factor. The rating factor represents the multiple of rating vehicles that the bridge can safely carry. Separate factors are computed for the different members and different load effects (i.e., moment, shear, etc.), with the smallest value controlling the rating.

In the AS and LF methods, each highway bridge is rated at an inventory and operating level. The inventory rating level corresponds to the customary design level of stresses and results in a live load that can safely utilize an existing structure for an indefinite period of time. On the other hand, the operating rating level is the maximum permissible live load to which a bridge may be subjected, but on a less frequent basis. These two ratings are reported in terms of the rating vehicle that was used to compute the

live load effects, which results in two values of the load rating RT, that is IR (Inventory Rating) and OR (Operating Rating). IR is the value to be used in the calculation for sufficient rating.

In the AS method, the dead load and live load factors (A_1 and A_2) are taken as unity, while the member capacity (C) is determined based on the rating level evaluated. For example, for reinforced concrete members, if the ultimate strength of the concrete is between 3000 psi and 3900 psi, the inventory and operating ratings are determined based on the maximum allowable bending stresses of 1200 psi and 1900 psi, respectively. On the other hand, in the LF method, the rating is determined such that the effect of the factored loads does not exceed the strength of the member. The dead load factor is taken as 1.3 whereas the live load factor is taken as 2.17 and 1.3 for inventory and operating ratings, respectively. The nominal capacity C remains the same regardless of the rating level, and in general, is calculated based on the AASHTO Design Specifications. It should also take into account the observable effects of deterioration, such as loss of concrete or steel-sectional area, loss of composite action and corrosion.

4.0 FRP Materials

4.1 Overview

Fiber reinforced polymers consist, as the name implies, of two basic materials: fibers and a polymeric resin. The fibers are encased in the resin and provide principally tensile strength, while the resin provides shear strength and transfers loads between the fibers. There are many different fibers and resins available. Each has their advantages and disadvantages. In addition to the different basic materials, there are also alternative methods to attach FRP to a structure.

FRP strengthening systems are essentially custom-made. They are not at this point commodities, and therefore the systems are all proprietary. Although the constituent materials can be combined in an ad hoc or smorgasbord manner, this is not at all recommended because of the uncertainty of the short and long-term performance. Therefore, a specific system needs sufficient test data to assure its performance (ACI, 2002).

The objective of this section is to provide a brief overview of the most significant materials and methods of application. The material herein is based heavily on ACI 440 (ACI, 2002) and Barr (2001).

4.2 Fibers

The three primary types of fibers used for structural strengthening applications are E-glass, aramid, and carbon. A review of previous strengthening projects indicates that where strength is important, carbon fiber is now a popular choice. Although more expensive than glass, it is stronger and stiffer, and it has better fatigue and creep characteristics (ACI, 2002).

The elastic moduli of fibers range from 32,000 to 100,000 ksi for carbon; 10,000 ksi for E-glass; and 10,000 to 18,000 ksi for aramid. The ultimate strengths are 200,000 to 900,000 ksi for carbon; 270,000 to 390,000 ksi for E-glass; and 500,000 to 600,000 for aramid (ACI, 2002). These values are provided to give a sense of the strength and stiffness of the FRP, not for use in design. Manufacturers' data should be referenced for design strengths.

4.3 Resins

The resins used for FRP are typically thermosetting resins, i.e., resins that permanently harden upon heating. Possible types of resins include epoxy, esters, polyesters, vinyl esters, and phenolic materials. Polyester, epoxy, and vinyl ester resins are particularly popular, and some of their characteristics are discussed below, based on Barr (2001).

Polyester resins are inexpensive and have been used for years in fiberglass. They are relatively inexpensive and well tested. However, they do not adhere to all surfaces well, and they are not the best at withstanding fatigue. In addition, styrene, a component of the resins, is volatile and produces hazardous vapors. Work areas must be well ventilated, and air quality requirements may negate its use.

Epoxy resins have several advantages over polyester resins. They adhere well to a larger variety of surfaces and they have good fatigue characteristics. In addition, they have much less problem with air emissions. They are, however, more expensive than polyesters.

Vinyl ester resin is a hybrid polyester/epoxy, and therefore it inherits characteristics from both of these resins. Although it is more resistant to fatigue than is polyester, it has similar toxic emissions problems.

4.4 Methods of Application

There are essentially three methods to apply FRP to a structure: wet lay-up, prepreg systems, and precured systems.

4.4.1 Wet Lay-Up Systems

A wet lay-up system involves dry fibers and in-place application and wetting of the fibers to the structure. Uni- and multi-directional fiber sheets are saturated on-site and applied to the structure. The saturating resin may also be used to bond the fiber to the concrete, or a second bonding resin may be used.

Wet lay-up systems are very flexible, in that they are easily molded to a variety of shapes. They are not pretensioned, and the final performance of the system depends very much on the quality of the installation. Care must be taken to ensure that wrinkles are removed from the sheets, or strength can be negatively impacted. Because of the wet

resin, application can be messy. Adequate ventilation is especially important for polyester and vinyl ester resins (Barr, 2001). Curing is obviously achieved on-site.

4.4.2 Prepreg Systems

Prepreg systems use fiber sheets impregnated with a resin off-site, at a manufacturing plant. Hence, these sheets typically have better quality control than do the wet lay-up systems. Either the impregnating resin or a second bonding resin is used to bond the sheets to the concrete. These systems are also cured on-site, and heating may be required (ACI, 2002).

4.4.3 Precured Systems

Precured systems are manufactured off-site. On-site, they require bonding to the concrete surface, for which an adhesive resin is used. Because these systems are cured in a manufacturing facility, quality control of the FRP is typically quite good. The weak link of these applications can be the bond between the FRP and the concrete, and good surface preparation is important. Pre-manufactured, thicker pultrusion plates can be used with this system. When applying this system, a roller may be needed to remove air bubbles between the plate and the concrete surface. As compared to the other two types, this system is more difficult to fit to an irregular surface (Barr, 2001).

5.0 Design of FRP Reinforcement

5.1 Overview

Design of FRP reinforcement is primarily based on the traditional steel reinforced concrete design principles stated in ACI 318. The contribution of FRP reinforcement is calculated by satisfying strain compatibility and internal force equilibrium based on the mechanical behavior of FRP reinforcements. Although FRP systems are effective in strengthening members in various modes of behavior, only flexural and shear strengthening will be considered in this report. Section 5.2 discusses the design principles, while sections 5.3 and 5.4 provide detailed discussions of design for flexural and shear strengthening, respectively. Section 5.5 discusses strategies of attaching the FRP to the concrete structure to ensure full action of the FRP strength.

5.2 Design Principles

The design procedure is based on the limit states design principles, in which potential modes of failure (limiting states) are identified and the design is carried out so that acceptable levels of safety are obtained against occurrence of each limit state. Limit states that are normally considered for reinforced concrete structures are ultimate limit states, such as rupture and fatigue, and serviceability limit states including excessive deflections and crack width. In each limit state, the resistance must exceed the load effects, and the acceptable safety levels are achieved by applying load factors (greater than one) and strength reduction factors (less than one) to load effects and resistance, respectively. This requirement can be expressed as

$$\phi R_n = \alpha_1 S_1 + \alpha_2 S_2 + \dots \quad (5.1)$$

where ϕ is the strength reduction factor; R_n is the nominal resistance; S_i are the individual load effects; and α_i are the associated load factors. Partial strength reduction factors are applied to the resistance contributed by the FRP reinforcement to reflect lesser existing knowledge of FRP systems compared to reinforced and prestressed concrete.

Strengthening limits are primarily governed by the capacity of the original structure without the contribution of the FRP system. This capacity should be capable of

continuing to support a certain level of load to guard against collapse of the structure should bond or other failure of the FRP system occur due to fire, vandalism, etc. ACI 440 (ACI, 2002) recommends that the strength of the original structure satisfy the equation:

$$\phi R_n = 1.2S_{DL} + 0.85S_{LL}$$

where S_{DL} and S_{LL} represent the dead and live load effects, respectively. Moreover, as FRP strengthening increases the member resistances associated with specific modes of failure only, such as flexure and shear, it is important to ensure that all components of the structure are capable of withstanding the increased level of load effects associated with the strengthened members.

5.3 Flexural Strengthening

An increase in flexural capacity can be obtained by bonding FRP reinforcement to the tension face of the concrete flexural member with fibers oriented along the length of the member. To maintain ductile behavior by ensuring that shear does not control failure, the FRP contribution to flexural capacity should be examined carefully.

5.3.1 General Assumptions

The following assumptions are made in calculating the flexural resistance of a section strengthened with an externally bonded FRP system.

- The strains in the reinforcement and concrete are directly proportional to the distance from the neutral axis.
- The FRP reinforcement is applied to the tension face of the concrete member.
- Perfect bond exists between the concrete and FRP reinforcement.
- The maximum compressive strain in the concrete is 0.003.
- The tensile strength of concrete is ignored.
- The FRP reinforcement has a linear elastic stress-strain relationship to failure.
- Substrate strain ε_{bi} due to the preexisting loading should be considered.

5.3.2 Ultimate Strength

The ultimate strength design criteria states that the design flexural capacity (nominal strength M_n multiplied by a strength reduction factor ϕ) of a member must exceed the flexural demand M_u (load effects calculated from factored loads):

$$\phi M_n \geq M_u \quad (5.2)$$

The nominal flexural capacity is computed based on strain compatibility and internal force equilibrium, considering the controlling mode of failure:

$$M_n = A_s f_s \left(d - \frac{\beta_1 c}{2} \right) + \psi_f A_f f_{fe} \left(h - \frac{\beta_1 c}{2} \right) \quad (5.3)$$

where

A_s : Area of steel reinforcement

f_s : Stress in steel reinforcement

d : Distance from the extreme compression fiber to the centroid of the steel reinforcement

β_1 : Ratio of the depth of equivalent rectangular stress block to the depth of the neutral axis

c : Distance from the extreme compression fiber to the neutral axis

ψ_f : Partial reduction factor for flexure

A_f : Area of FRP reinforcement

f_{fe} : Effective stress in FRP

h : Height of the member

ACI 440 recommends a partial reduction factor $\psi_f = 0.85$ for flexural strengthening.

The following failure modes should be investigated for an FRP strengthened section:

- Crushing of the concrete in compression before yielding of the reinforcing steel
- Yielding of the steel in tension followed by rupture of the FRP laminate

- Yielding of the steel in tension followed by concrete crushing
- Shear/tension delamination of the concrete cover
- Debonding of the FRP from the concrete substrate

Concrete crushing occurs if the compressive strain in the concrete reaches its maximum strain $\varepsilon_c = 0.003$. FRP rupture occurs if the strain in the FRP reaches its design rupture strain ($\varepsilon_f = \varepsilon_{fu}$)

5.3.3 Strain Compatibility

The strain in the FRP reinforcement at the ultimate state (concrete crushing) is:

$$\varepsilon_{fe} = 0.003 \left(\frac{h-c}{c} \right) - \varepsilon_{bi} \quad (5.4)$$

and the strain in the tension steel is:

$$\varepsilon_s = 0.003 \left(\frac{d-c}{c} \right) \quad (5.5)$$

5.3.4 Internal Force Equilibrium

The stress in the steel is:

$$f_s = E_s \varepsilon_s \leq f_y \quad (5.6)$$

and the stress level in the FRP reinforcement is:

$$f_{fe} = E_f \varepsilon_{fe} \quad (5.7)$$

where E_s and E_f are, respectively, the Young's modulus for the steel and FRP reinforcement, and f_y is the steel yield stress. Internal force equilibrium can be expressed as:

$$A_s f_s + A_f f_{fe} = \gamma f'_c \beta_1 c b \quad (5.8)$$

where b is the width of the rectangular concrete section. The depth to the neutral axis c is found by simultaneously satisfying the above five equations.

5.3.5 Design Example

Simple beam ($L = 15$ ft)

Concrete: $b = 5$ in.; $h = 14$ in.; $f'_c = 6000$ psi; $E_c = 57000\sqrt{f'_c} = 4415$ ksi

Steel: $A_s = 0.47$ in.²; $d = 13$ in.; $f_y = 60$ ksi; $E_s = 30000$ ksi

FRP: $A_f = 0.095$ in.²; $E_f = 22000$ ksi; $\epsilon_{fu} = 0.0155$

1. Determine existing substrate strain ϵ_{bi} due to dead load

Uniform dead load intensity: $w_D = \frac{5 \times 14}{144} \times 150 = 73$ lb/ft

Factored load: $1.4w_D = 102$ lb/ft

Maximum moment due to factored load: $M_{exist} = \frac{102 \times 15^2}{8} \times 12 = 34425$ in.-lb

Calculate yield moment M_y

Steel strain at yield: $\epsilon_{sy} = \frac{f_y}{E_s} = \frac{60}{30000} = 0.002$

Concrete strain at yield: $\epsilon_{cy} = \frac{c}{d-c} \epsilon_{sy}$

Compressive force = Tensile force:

$$\rightarrow A_s f_y = \frac{1}{2} b c E_c \epsilon_{cy}$$

$$\rightarrow 0.47 \times 60 = \frac{1}{2} \times 5 \times c \times 4414 \times \frac{c}{13-c} \times 0.002$$

$$\rightarrow c = 3.49 \text{ in.}$$

For this value of c , $\epsilon_{cy} = \frac{3.49}{13-3.49} \times 0.002 = 0.000734$ □ $\epsilon_{cu} = 0.003$ (OK)

$$\rightarrow M_y = A_s f_y \left(d - \frac{c}{3} \right) = 0.47 \times 60 \times \left(13 - \frac{3.49}{3} \right) = 334 \text{ in.-k}$$

Yield curvature: $\phi_y = \frac{\epsilon_{cy}}{c} = \frac{0.000734}{3.49} = 0.000210$ /in.

$$\rightarrow \phi_{exist} = \frac{M_{exist}}{M_y} \phi_y = \frac{34.4}{334} \times 0.000210 = 0.0000216 \text{ /in.}$$

Assume c at $M_{exist} = c$ at M_y

$$\rightarrow \epsilon_{bi} = (h - c)\phi_{exist} = (14 - 3.49) \times 0.0000216 = 0.000227$$

2. Determine c of the composite section

Assume the concrete crushing failure mode:

Since $f'_c = 6000$ psi, $\gamma = 0.85$; $\beta_1 = 0.75$

$$\text{FRP strain: } \epsilon_{fe} = \epsilon_{cu} \frac{h - c}{c} - \epsilon_{bi} = 0.003 \times \frac{14 - c}{c} - 0.000227$$

$$\rightarrow \text{FRP stress: } f_{fe} = E_f \epsilon_{fe}$$

Assume steel has not yielded:

$$\text{Steel strain: } \epsilon_s = \epsilon_{cu} \frac{d - c}{c} = 0.003 \times \frac{13 - c}{c}$$

$$\rightarrow \text{Steel stress: } f_s = E_s \epsilon_s$$

$$\text{Equilibrium: } A_s f_s + A_f f_{fe} = \gamma f'_c \beta_1 b c$$

$$\rightarrow 0.47 \times 30000 \times 0.003 \times \frac{13 - c}{c} + 0.095 \times 22000 \times \left(0.003 \times \frac{14 - c}{c} - 0.000227 \right)$$

$$= 0.85 \times 6 \times 0.75 \times 5 \times c$$

$$\rightarrow c = 4.63 \text{ in.}$$

$$\text{For this value of } c, \epsilon_s = 0.003 \times \frac{13 - 4.63}{4.63} = 0.00542 > \epsilon_y = 0.002 \text{ (Steel has yielded)}$$

$$\rightarrow \text{Steel stress} = f_y$$

$$\text{Equilibrium: } A_s f_y + A_f f_{fe} = \gamma f'_c \beta_1 b c$$

$$\rightarrow 0.47 \times 60 + 0.095 \times 22000 \times \left(0.003 \times \frac{14 - c}{c} - 0.000227 \right) = 0.85 \times 6 \times 0.75 \times 5 \times c$$

$$\rightarrow c = 2.78 \text{ in.}$$

$$\text{For this value of } c, \epsilon_s = 0.003 \times \frac{13 - 2.78}{2.78} = 0.0110 > \epsilon_y = 0.002 \text{ (OK)}$$

Check the level of FRP strain: $\varepsilon_{fe} = 0.003 \times \frac{14 - 2.78}{2.78} - 0.000227 = 0.0119 < \varepsilon_{fu} = 0.0155$

(OK)

$$\rightarrow f_{fe} = E_f \varepsilon_{fe} = 22000 \times 0.0119 = 261.8 \text{ k}$$

3. Capacity of the FRP-reinforced beam:

$$\begin{aligned} \text{Nominal capacity: } M_n &= A_s f_y \left(d - \frac{\beta_1 c}{2} \right) + \psi A_f f_{fe} \left(h - \frac{\beta_1 c}{2} \right) \\ &= 0.47 \times 60 \times \left(13 - \frac{0.75 \times 2.78}{2} \right) + 0.85 \times 0.095 \times 261.8 \times \left(14 - \frac{0.75 \times 2.78}{2} \right) \\ &= 611 \text{ in.-k} \end{aligned}$$

$$\rightarrow \text{Ultimate capacity: } \phi M_n = 0.9 \times 611 = 550 \text{ in.-k}$$

4. Capacity without FRP reinforcement

Equilibrium without FRP (assume steel has yielded): $A_s f_y = \gamma f'_c \beta_1 b c$

$$\rightarrow 0.47 \times 60 = 0.85 \times 6 \times 0.75 \times 5 \times c$$

$$\rightarrow c = 1.47 \text{ in.}$$

$$\begin{aligned} \rightarrow M_n &= A_s f_y \left(d - \frac{\beta_1 c}{2} \right) \\ &= 0.47 \times 60 \times \left(13 - \frac{0.75 \times 1.47}{2} \right) \\ &= 351 \text{ in.-k} \end{aligned}$$

$$\rightarrow \text{Ultimate capacity: } \phi M_n = 0.9 \times 351 = 316 \text{ in.-k}$$

The gain in flexural strength due to FRP reinforcement is 74%.

5. Case in which ε_{bi} is neglected

$$\text{FRP strain: } \varepsilon_{fe} = \varepsilon_{cu} \frac{h - c}{c} = 0.003 \times \frac{14 - c}{c}$$

Assume the steel has yielded.

$$\text{Equilibrium: } A_s f_y + A_f f_{fe} = \gamma f'_c \beta_1 b c$$

$$\rightarrow 0.47 \times 60 + 0.095 \times 22000 \times 0.003 \times \frac{14 - c}{c} = 0.85 \times 6 \times 0.75 \times 5 \times c$$

$$\rightarrow c = 2.79 \text{ in.}$$

$$\text{Check the level of FRP strain: } \varepsilon_{fe} = 0.003 \times \frac{14 - 2.79}{2.79} = 0.0121 < \varepsilon_{fu} = 0.0155 \quad (\text{OK})$$

$$\rightarrow f_{fe} = E_f \varepsilon_{fe} = 22000 \times 0.0121 = 266.2 \text{ k}$$

$$\begin{aligned} \text{Nominal capacity: } M_n &= A_s f_y \left(d - \frac{\beta_1 c}{2} \right) + \psi A_f f_{fe} \left(h - \frac{\beta_1 c}{2} \right) \\ &= 0.47 \times 60 \times \left(13 - \frac{0.75 \times 2.79}{2} \right) + 0.85 \times 0.095 \times 266.2 \times \left(14 - \frac{0.75 \times 2.79}{2} \right) \\ &= 616 \text{ in.-k} \end{aligned}$$

$$\rightarrow \text{Ultimate capacity: } \phi M_n = 0.9 \times 616 = 554 \text{ in.-k}$$

Although the result is not conservative, the difference is negligible.

5.4 Shear Strengthening

Applying FRP as external stirrups can increase the shear strength of existing concrete beams. Although it is most efficient to orient the FRP fibers perpendicular to potential shear cracks, for practical reasons the fibers can be oriented transverse to the axis of the member. Increasing the shear strength is pivotal in enhancing the overall load-carrying capacity, as flexural strengthening only would lead to the brittle failure associated with shear.

5.4.1 Wrapping Schemes

Completely wrapping the section on all four sides is the most effective wrapping scheme, and will, in general, lead to the greatest increase in shear capacity (Figure 5-1). Special preparations such as making holes in the member become necessary when this wrapping scheme is applied to a beam with a slab on it (Figure 5-1 (b)), or to a prestressed beam which normally has a reduced cross section for the web (Figure 5-1 (c)). Shear strength can also be improved by wrapping three sides of the member (Figure 5-2 (a)) or bonding to the two sides of the member (Figure 5-1 (b)). However, these two schemes do not take full advantage of the FRP stirrups and normally result in a less amount of increase in load-carrying capacity as compared to the complete wrapping

scheme. This is primarily due to the FRP stirrups not being properly anchored in the compression zone as required by ACI 318 in the case of steel stirrups.

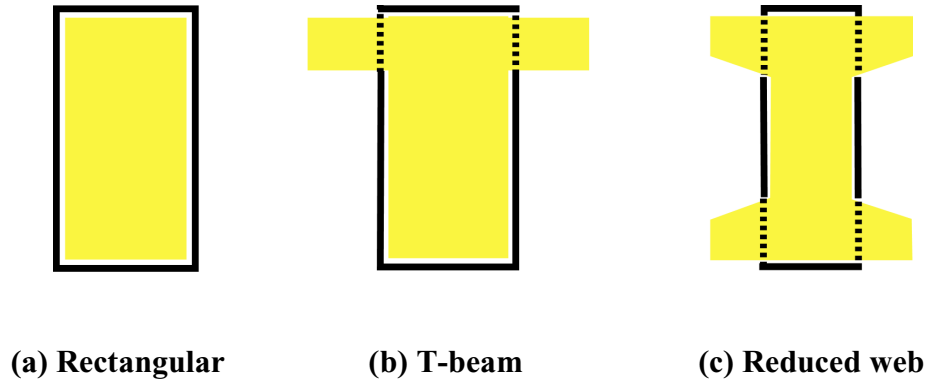


Figure 5-1: Complete wrapping

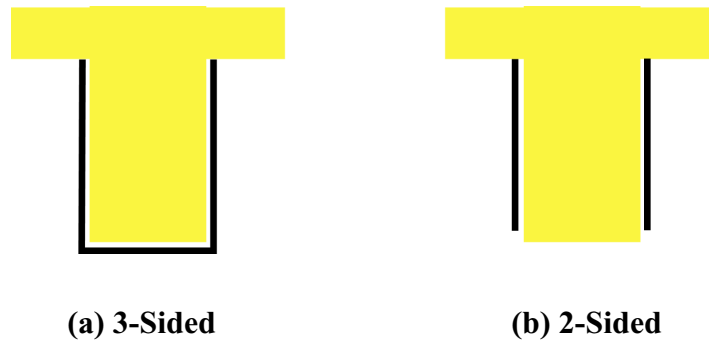


Figure 5-2: Partial wrapping

5.4.2 Ultimate Strength

The ultimate strength design criteria state that the design shear capacity (nominal strength V_n multiplied by a strength reduction factor ϕ) of a member must exceed the shear demand V_u (load effects calculated from factored loads):

$$\phi V_n \geq V_u \tag{5.9}$$

The nominal shear capacity of a FRP strengthened member is the summation of the contributions from concrete, reinforcing steel, and FRP:

$$\phi V_n = \phi(V_c + V_s) + \phi_f V_f \quad (5.10)$$

where ϕ_f is the reduction factor applied to the contribution of the FRP reinforcement.

5.4.3 Shear Strength by FRP Reinforcement

Shear strength provided by FRP can be determined based on two possible failure modes, and the lower of the two results is taken as the shear strength contribution of the FRP reinforcement. The two failure modes considered are FRP rupture and delamination, or debonding of the FRP from the concrete surface. A literature review indicates that the contribution of FRP to shear strength at present can only be approximated. Presented here are two possible procedures, which are based on a calibration with available test data.

5.4.3.1 Procedure by Khalifa et al. (1998)

1. Shear Strength Based on FRP Rupture

The shear strength can be determined by calculating the force resulting from the tensile stress in the FRP along the assumed crack:

$$V_f = \frac{A_{fv} f_{fe} (\sin \alpha + \cos \alpha) d_f}{s_f} \quad (5.11)$$

where

$A_{fv} = 2nt_f w_f$: FRP shear reinforcement area in spacing s_f

n : No. of FRP plies

t_f : FRP thickness

w_f : FRP width

$f_{fe} = E_f \varepsilon_{fe}$: FRP effective stress

α : Angle of inclination of stirrups

d_f : Depth of FRP reinforcement

FRP rupture occurs at an average stress level that is below the ultimate strength of FRP due to stress concentration. In order to explain this phenomenon, the effective strain, which is less than the ultimate strain ε_{fu} , is computed as:

$$\varepsilon_{fe} = R\varepsilon_{fu} \quad (5.12)$$

where the reduction factor R is determined by

$$R = 2.674 \times 10^{-5} (\rho_f E_f)^2 - 8.406 \times 10^{-3} (\rho_f E_f) + 0.778 \leq 0.50$$

Here the FRP modulus E_f is given in ksi, and the FRP shear reinforcement ratio is defined as:

$$\rho_f = \frac{2t_f w_f}{bs_f} \quad (5.13)$$

2. Shear Strength Based on FRP Delamination

Delamination of the FRP from the concrete surface is the failure related to the bond mechanism, and is more applicable to the FRP systems that do not close around the entire cross section. This is due to the nature of the wrapping schemes where all four sides are not completely wrapped, which leads to reduced bonding between the FRP and concrete surface. Although recommended for CFRP only due to the limited experimental results available, the shear strength based on this failure mode can be obtained by the approach based on the concepts of effective bond length and average bond stress as:

$$V_f = \frac{P_{\max} w_{fe}}{s_f} \quad (5.14)$$

Thus, the shear strength based on the bond mechanism employs, instead of $A_{fv} f_{fe}$ as in the failure mode associated with FRP delamination, the ultimate load capacity of the CFRP sheet P_{\max} defined as:

$$P_{\max} = 2L_e w_f \tau_{bu} \quad (5.15)$$

where

$L_e = e^{3.910-0.58\ln(t_f E_f)}$: Effective bond length (in.)

$$\tau_{bu} = 2.80 \times 10^{-3} \left(\frac{f'_c}{6000} \right)^{2/3} E_f t_f : \text{Average bond stress (ksi)}$$

When the above equations are used, the FRP thickness and the concrete strength are given in in. and psi, respectively. Effective FRP width w_{fe} is used in place of d_f recognizing that once a shear crack develops, only that portion of FRP extending past the crack by the effective bonded length will be capable of carrying shear:

$$w_{fe} = d_f \quad \text{Complete wrapping}$$

$$w_{fe} = d_f - L_e \quad \text{U-wrap}$$

$$w_{fe} = d_f - 2L_e \quad \text{Two sides}$$

Finally, the nominal shear strength is calculated as $\phi_f V_f$, where ϕ_f is taken equal to 0.70.

5.4.3.2 Procedure by Triantafillou and Antonopoulos (2000)

In this procedure, the FRP shear strength is calculated with the same equation used in Khalifa's procedure:

$$V_f = \frac{A_{fv} f_{fe} (\sin \alpha + \cos \alpha) d_f}{s_f} \quad (5.16)$$

where

$$f_{fe} = E_f \varepsilon_{fe,A} \quad (5.17)$$

with $\varepsilon_{fe,A} = 0.9 \varepsilon_{fe} \leq 0.006$. For fully wrapped CFRP, shear failure is mainly governed by FRP rupture, and the corresponding effective strain ε_{fe} is

$$\varepsilon_{fe} = 0.28 \left(\frac{f'_c}{\rho_f E_f} \right)^{0.30} \varepsilon_{fu} \quad (5.18)$$

For the other wrapping schemes (U-wrap or two sides), not only the above failure mode but also the failure due to FRP delamination needs to be considered, for which

$$\varepsilon_{fe} = 1.65 \left(\frac{f_c'^{2/3}}{\rho_f E_f} \right)^{0.56} \times 10^{-3} \quad (5.19)$$

$\phi_f = 0.75$ is used if FRP debonding dominates while $\phi_f = 0.80$ is recommended if the failure is governed by FRP fracture. $\phi_f = 0.75$ is used if $\varepsilon_{fe,A} = \varepsilon_{\max} = 0.006$.

5.4.4 Design Example

Concrete: $b = 5$ in.; $h = 14$ in.; $f_c' = 6000$ psi; $E_c = 57000\sqrt{f_c'} = 4415$ ksi

Steel shear stirrup: $A_v = 0.22$ in.²; $d = 13$ in.; $f_y = 60$ ksi; $E_s = 30000$ ksi

FRP shear stirrup: CFRP U-wrap; $E_f = 22000$ ksi; $\varepsilon_{fu} = 0.0155$; $t_f = 0.0065$ in.

Continuous strips $\rightarrow s_f = w_f$

Angle of fiber orientation = 90°

1. Concrete

Concrete shear strength: $V_c = 2\sqrt{f_c'} b_w d = 2\sqrt{6000} \times 5 \times 13 = 10.1$ k

2. Steel

Steel shear strength: $V_s = \frac{A_v f_y d}{s} = \frac{0.22 \times 60 \times 13}{9} = 19.1$ k

3. FRP

Procedure by Khalifa et al.

a. FRP rupture failure mode

FRP shear reinforcement ratio: $\rho_f = \frac{2t_f w_f}{bs_f} = \frac{2 \times 0.0065}{5} = 0.0026$

$\rightarrow \rho_f E_f = 0.0026 \times 22000 = 57.2$ ksi

$$\begin{aligned} \rightarrow \text{Reduction factor: } R &= 2.674 \times 10^{-5} (\rho_f E_f)^2 - 8.406 \times 10^{-3} (\rho_f E_f) + 0.778 \\ &= 2.674 \times 10^{-5} (57.2)^2 - 8.406 \times 10^{-3} (57.2) + 0.778 \\ &= 0.38 < 0.50 \quad (\text{OK}) \end{aligned}$$

$$\rightarrow \text{FRP effective stress: } f_{fe} = RE_f \varepsilon_{fu} = 0.38 \times 22000 \times 0.0155 = 130 \text{ ksi}$$

Since FRP sheets are applied on both sides, $A_{fv} = 2t_f w_f$

$$\rightarrow \text{FRP shear strength: } V_f = \frac{A_{fv} f_{fe} (\sin \alpha + \cos \alpha) d_f}{s_f} = \frac{2 \times 0.0065 \times w_f \times 130 \times 13}{s_f} = 22.0 \text{ k}$$

b. FRP delamination failure mode

$$\text{Effective bond length: } L_e = e^{3.910 - 0.58 \ln(t_f E_f)} = e^{3.910 - 0.58 \ln(0.0065 \times 22000)} = 2.81 \text{ in.}$$

$$\begin{aligned} \text{Average bond stress: } \tau_{bu} &= 2.80 \times 10^{-3} \left(\frac{f'_c}{6000} \right)^{2/3} E_f t_f \\ &= 2.80 \times 10^{-3} \left(\frac{6000}{6000} \right)^{2/3} \times 22000 \times 0.0065 = 0.40 \text{ ksi} \end{aligned}$$

For U-wrap scheme, effective FRP width: $w_{fe} = d_f - L_e = 13 - 2.81 = 10.19 \text{ in.}$

$$\rightarrow \text{FRP shear strength: } V_f = \frac{2L_e w_f \tau_{bu} w_{fe}}{s_f} = \frac{2 \times 2.81 \times w_f \times 0.40 \times 10.19}{s_f} = 22.9 \text{ k}$$

Thus, FRP rupture failure mode controls.

$$\rightarrow V_f = 22.0 \text{ k}$$

$$\rightarrow \text{Ultimate capacity: } \phi V_n = \phi(V_c + V_s) + \phi_f V_f = 0.85 \times (10.1 + 22.0) + 0.70 \times 22.0 = 42.7 \text{ k}$$

The capacity without FRP reinforcement: $\phi V_n = \phi(V_c + V_s) = 27.3 \text{ k}$

The gain in shear strength due to FRP reinforcement is 56%.

Procedure by Triantafillou and Antonopoulos

a. FRP rupture failure mode

$$\text{FRP effective strain: } \varepsilon_{fe} = 0.28 \left(\frac{f'_c}{\rho_f E_f} \right)^{0.30} \varepsilon_{fu}$$

$$= 0.28 \left(\frac{6000^{2/3}}{57.2} \right)^{0.30} \times 0.0155 = 0.00734$$

b. FRP delamination failure mode

$$\begin{aligned} \text{FRP effective strain: } \varepsilon_{fe} &= 1.65 \left(\frac{f_c^{2/3}}{\rho_f E_f} \right)^{0.56} \times 10^{-3} \\ &= 1.65 \left(\frac{6000^{2/3}}{57.2} \right)^{0.56} \times 10^{-3} = 0.00440 \end{aligned}$$

Thus, FRP delamination failure mode controls ($\phi_f = 0.75$ is used).

$$\rightarrow \varepsilon_{fe,A} = 0.9 \varepsilon_{fe} = 0.9 \times 0.00440 = 0.00396 \leq 0.006 \text{ (OK)}$$

$$\rightarrow \text{FRP effective stress: } f_{fe} = E_f \varepsilon_{fe,A} = 22000 \times 0.00396 = 87.1 \text{ ksi}$$

$$\rightarrow \text{FRP shear strength: } V_f = \frac{A_{fv} f_{fe} (\sin \alpha + \cos \alpha) d_f}{s_f} = \frac{2 \times 0.0065 \times w_f \times 87.1 \times 13}{s_f} = 14.7 \text{ k}$$

$$\rightarrow \text{Ultimate capacity: } \phi V_n = \phi(V_c + V_s) + \phi_f V_f = 0.85 \times (10.1 + 22.0) + 0.75 \times 14.7 = 38.3 \text{ k}$$

$$\text{The capacity without FRP reinforcement: } \phi V_n = \phi(V_c + V_s) = 27.3 \text{ k}$$

The gain in shear strength due to FRP reinforcement is 40%.

5.5 Typical Bridge Applications

There are a large number of different historical concrete bridge structures in Hawaii. However, three common structural systems are used in most of these bridges. These include poured-in-place T-beams, precast AASHTO-type girders, and poured-in-place multi-cell box girders. The following sections provide suggested procedures for retrofitting these three types of bridge girder for flexural and shear strengthening.

5.5.1 Poured-in-place T-beam Bridges

A typical poured-in-place T-beam bridge is shown in Figure 5-3. The soffit of the T-beam girders may be level (Figure 5-4) or sloped/curved upwards (Figure 5-5).



Figure 5-3: Elevation of typical T-beam bridge



Figure 5-4: T-beam girders with level beam soffits



Figure 5-5: T-beam girders with sloped soffits

FRP flexural strengthening of these girders will involve the addition of FRP strips to the soffit of the webs as shown in Figure 5-6. Adequate anchorage must be provided at the ends of these strips and at reentrant corners to prevent peeling under tensile load. One form of anchorage using FRP wraps is shown in the figure.

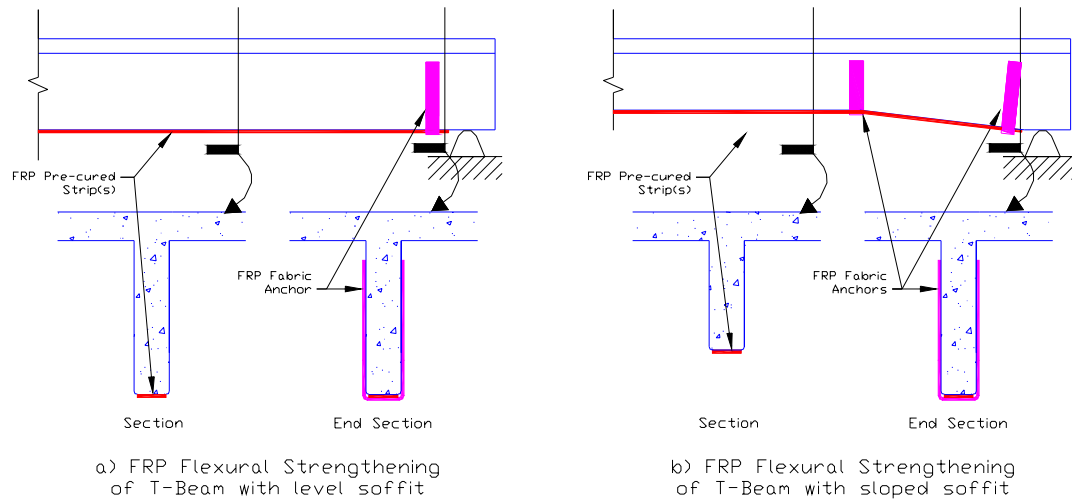


Figure 5-6: Typical flexural strengthening of T-beam bridge

Two alternatives for FRP shear strengthening of T-beam girders are shown in Figure 5-7. Ideally, closed stirrups of FRP are created as shown in Figure 5-7a. This requires breaking through the top slab of the bridge, with the associated disruption to traffic. If this is not possible, the stirrups or FRP sheets can be anchored at the soffit of the top slab by means of FRP or steel angles and through-bolts as shown in Figure 5-7b.

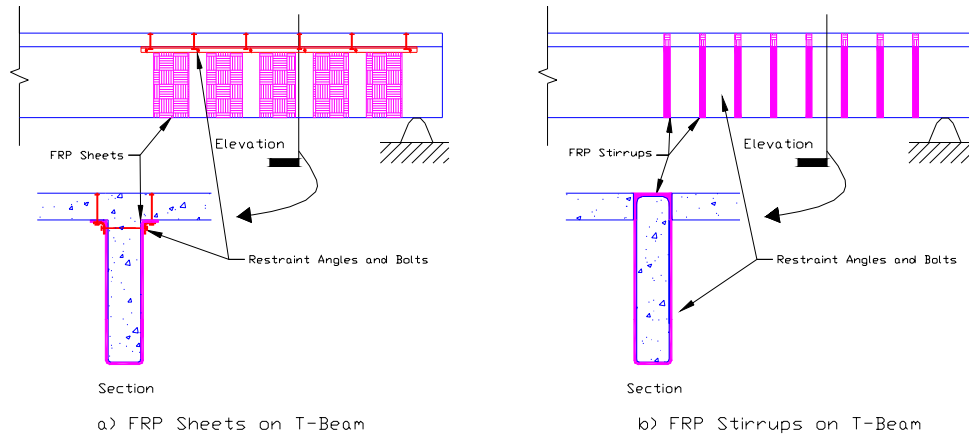


Figure 5-7: Typical shear strengthening of T-beam bridge

5.5.2 Precast AASHTO-Type Girder Bridges

A typical AASHTO-type girder bridge is shown in Figure 5-8 and Figure 5-9.



Figure 5-8: Elevation of typical AASHTO-type girder bridge



Figure 5-9: AASHTO-type girders

FRP flexural strengthening of these girders is similar to the T-beam girder described above. It will involve the addition of FRP strips to the soffit of the beam bulb as shown in Figure 5-10. Adequate anchorage must be provided at the ends of these strips. One form of anchorage using FRP wraps is shown in the figure.

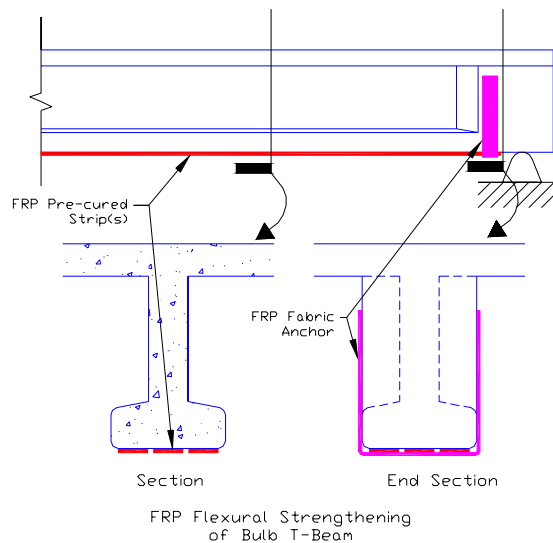


Figure 5-10: Typical flexural strengthening of AASHTO-type girder bridge

Two alternatives for FRP shear strengthening of AASHTO-type girders are shown in Figure 5-11. Ideally, closed stirrups of FRP are created as shown in Figure 5-11a. Because of the tendency of the reentrant corner at the top of the bulb to pull away from the concrete surface, it is necessary to provide a physical restraint such as the angle and bolts shown in Figure 5-11a. The top of the stirrups requires breaking through the top slab of the bridge, with the associated disruption to traffic. If this is not possible, the stirrups or FRP sheets can be anchored at the soffit of the top slab as shown in Figure 5-11b.

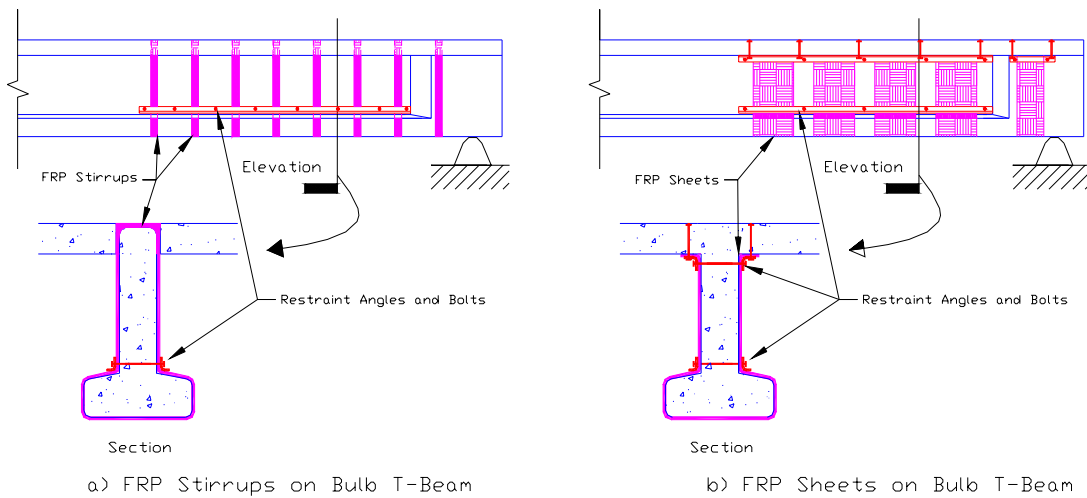


Figure 5-11: Typical shear strengthening of AASHTO-type girder bridge

5.5.3 Multi-cell Box Girder Bridges

A typical poured-in-place multi-cell box girder bridge is shown in Figure 5-12.



Figure 5-12: Typical multi-cell box girder bridge

FRP flexural strengthening of these girders will involve the addition of FRP strips to the soffit of the webs as shown in Figure 5-13. Adequate anchorage must be provided at the ends of these strips. One form of anchorage using FRP wrap is shown in the figure.

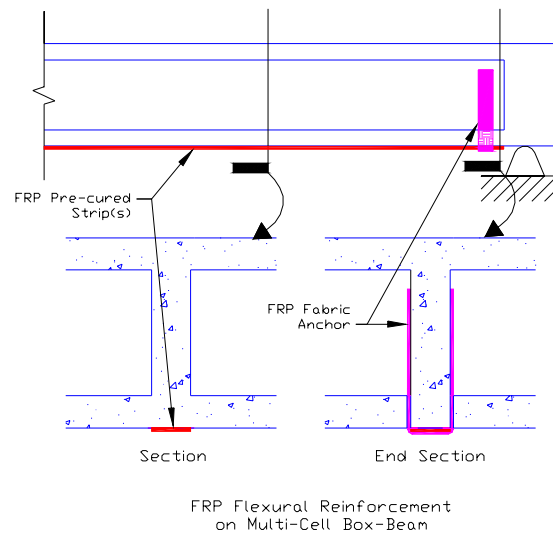


Figure 5-13: Typical flexural strengthening of multi-cell box girder bridge

Two alternatives for FRP shear strengthening of multi-cell box girders are shown in Figure 5-14. Ideally, closed stirrups of FRP are created as shown in Figure 5-14a. This requires breaking through the top and bottom slab of the bridge, with the associated

disruption to traffic. If this is not possible, the stirrups or FRP sheets can be anchored at the top and bottom of the webs as shown in Figure 5-14b.

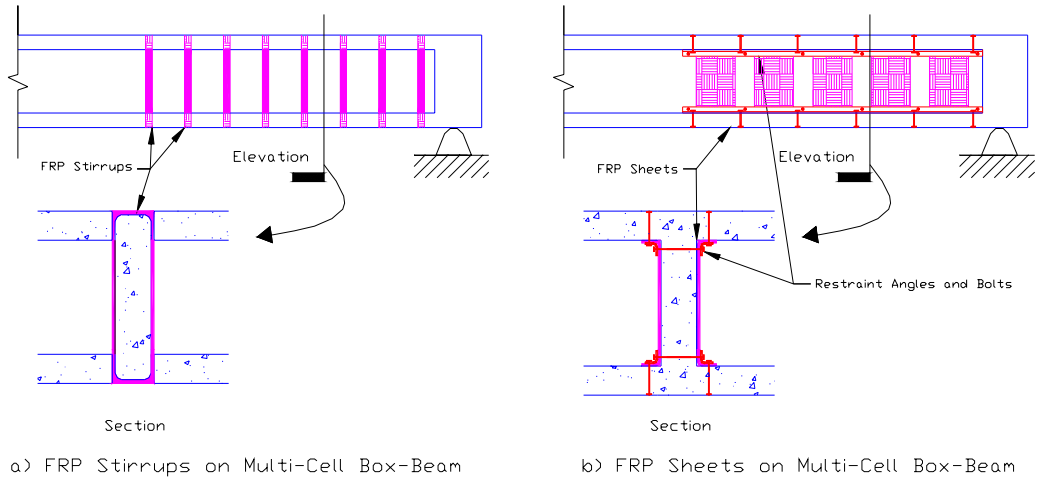


Figure 5-14: Typical shear strengthening of multi-cell box girder bridge

6.0 Application Procedures

6.1 Overview

This chapter provides a Guideline Specification for application of FRP retrofit materials to reinforced or prestressed concrete members for flexural and/or shear strengthening. This guideline covers only the specifications related to application of the FRP materials, and is not intended as a stand-alone specification for the project as a whole. General and other specifications should be included as required for the particular project.

Each suggested specification item is given in CAPITAL letters, followed in some cases by a commentary explaining the relevance of the item. It must be noted that these are only suggested specifications and that the project engineer of record (EOR) is ultimately responsible for the specifications provided for a particular project. As such, the EOR should modify these suggested specifications as required to suit each specific project.

These specifications were developed based on input from Brian Ide, a structural engineer with Allison Ide Engineers; Adriano ‘AB’ Bortelin, an engineering representative for Sika Products, a supplier of FRP products and systems; and Chandler Rowe of Plas-Tech Inc, a certified and experienced FRP system applicator in the State of Hawaii. Their contributions to this chapter are greatly appreciated.

6.2 Specification Overview

FRP retrofit systems are available from a number of manufacturers. Generally the contractor will be permitted to select a suitable system for the project based on specific performance criteria given in the specifications. In some cases the EOR may want to specify a particular type of FRP system or even a particular manufacturer; however, this precludes competitive bidding between manufacturers. It is very important that a complete system be used in each application. Combining a fiber fabric from one manufacturer with epoxies from another should never be permitted. Preparation of epoxies, fibers, and installation of the FRP system must follow the manufacturer’s specifications for the system and application in question.

Surface preparation and verification are important to the future performance of the FRP system. Verification of adequate surface preparation and testing of the materials and application integrity are also important components of these specifications.

6.3 Guideline Specification

PART 1 – GENERAL

- 1.01 THE CONTRACTOR OR HIS SUB-CONTRACTOR SHALL FURNISH ALL MATERIALS, TOOLS, EQUIPMENT, APPLIANCES, TRANSPORTATION, LABOR AND SUPERVISION REQUIRED TO PROPERLY INSTALL THE FRP MATERIALS COVERED BY THIS SPECIFICATION.
- 1.02 THE CONTRACTOR SHALL BE RESPONSIBLE FOR THE PROPER STORAGE, HANDLING, SAFETY CONSIDERATIONS AND DISPOSAL OF ANY HAZARDOUS MATERIALS INVOLVED IN THE FRP APPLICATION.
- 1.03 THE FRP APPLICATION SHALL BE PERFORMED BY AN APPLICATOR WITH PROVEN PAST EXPERIENCE UTILIZING THE SPECIFIC FRP SYSTEMS PROPOSED FOR THIS PROJECT.

Many FRP manufacturers/suppliers will only warrant their system if it is installed by an applicator specifically certified to install their products. It may be necessary to add this requirement in the above specification. The main FRP suppliers will generally have one or more pre-certified applicator in most areas of the country, including Hawaii.

- 1.04 THE FRP APPLICATOR SHALL SUBMIT A DETAILED WRITTEN DESCRIPTION OF THE PROPOSED FRP APPLICATION INCLUDING MATERIAL PROPERTIES AND APPLICATION PROCEDURES FOR REVIEW BY THE STRUCTURAL ENGINEER.

The structural engineer (EOR) must review the proposed application to ensure compliance with the requirements of the project documents. Once approved, the description is forwarded to the independent quality control personnel charged with oversight of the FRP application. It is important that the application procedure be followed precisely to ensure correct installation. Any changes to the procedure must be approved in writing by the EOR.

1.05 SUBMITTALS:

1.05.1 PRODUCT DATA: WITHIN SEVEN (7) CALENDAR DAYS AFTER THE CONTRACTOR HAS RECEIVED THE OWNER'S NOTICE TO PROCEED, SUBMIT THE FOLLOWING;

1.05.1.1 MATERIAL LIST OF ITEMS PROPOSED TO BE PROVIDED UNDER THIS SECTION.

1.05.1.2 MANUFACTURER'S SPECIFICATIONS AND OTHER DATA NEEDED TO PROVE COMPLIANCE WITH THE SPECIFIED REQUIREMENTS. THE MANUFACTURER'S SPECIFICATIONS SHALL INCLUDE PROCEDURES TO PROPERLY MIX THE INDIVIDUAL COMPONENTS OF THE PROPOSED PRODUCT AS WELL AS THE PROPER MIX RATIOS, ANTICIPATED POT LIFE AND ANY OTHER RELEVANT INFORMATION ABOUT THE PRODUCTS BEING USED.

1.05.1.3 MANUFACTURER'S RECOMMENDATIONS FOR SURFACE PREPARATION OF THE EXISTING CONCRETE SURFACE.

1.05.1.4 DETAILED WRITTEN DESCRIPTION OF THE PROPOSED MATERIAL APPLICATION PROCEDURES.

This information is reviewed by the EOR for completeness and compliance with the project requirements.

1.06 A SPECIAL INSPECTOR SHALL BE RETAINED BY THE CLIENT TO PROVIDE QUALITY ASSURANCE DURING INSTALLATION OF THE FRP COMPOSITE. THE SPECIAL INSPECTOR SHALL BE EXPERIENCED IN THE EVALUATION OF CONCRETE SURFACE PREPARATION, PERFORMANCE OF PULL-TESTS AND INSPECTION OF FRP APPLICATION.

It is recommended that the client hire an independent experienced inspector to provide quality assurance during FRP installation. The inspector would not need to be on site continuously, but would be responsible for inspecting surface preparation prior to FRP application, observing resin mixing and handling procedures, inspecting for bubbles or delamination after application, and performing all pull-tests required by these specifications.

PART 2 – MATERIALS AND EQUIPMENT

This section should contain basic material property requirements of the FRP system being specified. If no specific FRP system is identified in the contract documents, then this section will include only the general requirements to be satisfied in order for the strengthening to perform its intended function. If a particular FRP system is called for in the contract documents, then this section of the specification will be more specific. An example of the latter condition is given here:

2.01 CARBON FIBER/EPOXY MATRIX COMPOSITE SHALL HAVE THE FOLLOWING PROPERTIES:

2.02 LAMINATED PULTRUDED STRIPS

- ULTIMATE TENSILE STRENGTH (EFFECTIVE) = 406 KSI (MIN.)
- MODULUS OF ELASTICITY (EFFECTIVE) = 23,900 KSI (MIN.)
- ULTIMATE STRAIN = 1.9 % (MIN.)

2.03 20 OZ./SQ. YD. UNIDIRECTIONAL FABRIC; 0.047 INCH NOMINAL THICKNESS

- ULTIMATE TENSILE STRENGTH (EFFECTIVE) = 130 KSI
- MODULUS OF ELASTICITY (EFFECTIVE) = 10,900 KSI
- ULTIMATE STRAIN = 1.2 %

PART 3 – EXECUTION OF THE WORK

Surface preparation is a critical step in the application of FRP composites to concrete surfaces. For the tension and shear strengthening covered in this report, bond between the FRP material and the concrete substrate is critical. The specifications provided here are intended for these applications. Other applications, such as column wrapping, are considered contact critical, in which case the surface preparation may be less critical.

Surface preparation is often the most labor intensive and time consuming portion of the FRP application. As such, it is important that the specifications not be unnecessarily stringent. In addition, the condition of the concrete substrate may vary significantly between projects, so a standard surface preparation specification may not be suitable or appropriate for all projects. Trial surface preparation, confirmed by pull-tests, may be a

more appropriate means to establish the actual surface preparation required for a particular project.

It is strongly recommended that pull-tests be performed to verify the surface preparation prior to any FRP application. If pull-tests are performed only on the completed FRP system, and the results demonstrate inadequate surface preparation, repair or replacement of the entire FRP application would be extremely expensive, time consuming, and undesirable for all concerned. A representative sample area with satisfactory surface preparation should be maintained throughout the project for reference purposes.

The engineer may still require that a limited number of pull-tests be performed after application of the FRP to verify correct epoxy preparation and FRP application.

3 EXECUTION OF THE WORK

3.01 ALL CONCRETE SURFACES RECEIVING FRP OVERLAY SHALL BE PREPARED IN ACCORDANCE WITH RECOMMENDATIONS OF ACI 546R AND ICRI 03730, AS OUTLINED BELOW:

3.01.1 REMOVE ALL SURFACE PASTE OR CREAM TO EXPOSE THE COARSE AGGREGATE. THIS CAN BE ACHIEVED BY GRINDING, SHOT OR ABRASIVE BLASTING, OR SCARIFYING.

3.01.2 FINAL SURFACE PROFILE SHALL BE EQUIVALENT TO CSP3 OR BETTER AS DEFINED BY THE INTERNATIONAL CONCRETE REPAIR INSTITUTE (ICRI 03730). A CSP3 PROFILE SAMPLE MUST BE AVAILABLE ON SITE FOR THE DURATION OF THE PROJECT.

3.01.3 THE SURFACE SHALL BE FREE OF MOISTURE, DUST, GREASE, WAXES OR OTHER DELETERIOUS MATERIAL WHICH MAY INHIBIT BOND. THE SURFACE MUST BE PROTECTED FROM CONTAMINATION BY SUCH MATERIALS UNTIL APPLICATION OF THE FRP COMPOSITE.

3.01.4 PRIOR TO INSTALLATION OF ANY FRP COMPOSITE, PULL TESTS SHALL BE PERFORMED ON THE PREPARED SURFACE AT LOCATIONS SPECIFIED BY THE SPECIAL INSPECTOR IN ACCORDANCE WITH ACI 503R OR ASTM D 4541. THE PULL TEST PLUG SHALL BE BONDED TO THE PREPARED CONCRETE SURFACE

USING THE SAME EPOXY AS THE FINAL FRP APPLICATION. PULL TESTS SHALL BE PERFORMED WITH A PROCEQ DYNA-TESTER OR EQUIVALENT APPROVED TESTER, AND MUST PROVIDE A MINIMUM TENSILE CAPACITY OF 200 PSI AND EXHIBIT FAILURE OF THE CONCRETE SUBSTRATE.

3.01.5 IF PULL-TEST REQUIREMENTS ARE NOT MET, ADDITIONAL SURFACE PREPARATION SHALL BE PERFORMED UNTIL THE PULL-TEST RESULTS ARE SATISFACTORY.

3.01.6 A REFERENCE AREA OF PREPARED CONCRETE SURFACE SHALL BE RETAINED THROUGHOUT THE PROJECT AS A SAMPLE FOR EVALUATION OF NEW SURFACE PREPARATION. PULL-TESTS SHOULD BE PERFORMED ON THIS REFERENCE AREA TO ENSURE IT PROVIDES THE REQUIRED BOND CHARACTERISTICS.

3.01.7 REPAIR ALL DAMAGED CONCRETE, SPALLS, AND IRREGULAR SURFACES TO CREATE A SURFACE SUITABLE TO RECEIVE THE FRP COMPOSITE. REPAIR MATERIAL MAY BE POLYMER-MODIFIED PORTLAND CEMENT PATCHING MORTAR OR EPOXY-MODIFIED PATCHING MORTAR.

Application of the FRP system should follow the pre-approved manufacturer's directions precisely. If a particular FRP system has been selected for the project, it may be appropriate to include the manufacturer's application procedures in the specifications.

3.02 APPLY FRP MATERIALS IN STRICT COMPLIANCE WITH MANUFACTURER'S DIRECTIONS AS APPROVED BY THE ENGINEER.

3.03 WHERE REQUIRED, A #30 GRIT SAND SHALL BE BROADCAST ONTO THE FINAL COAT OF THE EPOXY MATRIX TO LEAVE A SURFACE WHICH IS CAPABLE OF ACCEPTING THE APPROPRIATE ARCHITECTURAL FINISH.

3.04 THE CONTRACTOR SHALL PROVIDE TEST COUPONS OF THE FRP COMPOSITE FOR TESTING. THE COMPOSITE COUPONS SHALL BE PREPARED IN THE SAME MANNER AS THE COMPOSITE OVERLAY FOR THE SLAB EXCEPT THAT A PLASTIC COVERED 1'-0" X 1'-0" SHEET OF PLYWOOD SHALL BE USED AS A BASE. AFTER THE COMPOSITE OVERLAY HAS CURED, FIVE TEST COUPONS REPRESENTATIVE OF THE ACTUAL LAY-UP SHALL BE CUT AND TESTED BY AN APPROVED TESTING LABORATORY IN ACCORDANCE WITH ASTM D 3039 TO PROVIDE:

- ULTIMATE TENSILE STRENGTH
- MODULUS OF ELASTICITY
- ULTIMATE STRAIN.

- 3.05 SELECTION OF THE TESTING LABORATORY AND THE COST OF TESTING SHALL BE THE RESPONSIBILITY OF THE CLIENT.
- 3.06 ALL BUBBLES AND DELAMINATIONS SHALL BE REPAIRED AS DIRECTED BY THE ENGINEER. SMALL DELAMINATIONS MAY BE ACCEPTABLE WITHOUT REPAIR, OR MAY REQUIRE INJECTION WITH EPOXY TO FILL THE DELAMINATION VOID. LARGER DELAMINATIONS MAY NEED TO BE REPAIRED BY CUTTING OUT THE DELAMINATED AREA AND PATCHING WITH ADEQUATE LAP LENGTHS.
- 3.07 IF REQUIRED BY THE ENGINEER, PULL TESTS SHALL BE PERFORMED ON THE COMPLETED FRP COMPOSITE INSTALLATION AT LOCATIONS SPECIFIED BY THE SPECIAL INSPECTOR IN ACCORDANCE WITH ACI 503R OR ASTM D 4541. PULL TESTS MUST PROVIDE A MINIMUM TENSILE CAPACITY OF 200 PSI AND EXHIBIT FAILURE OF THE CONCRETE SUBSTRATE. TEST AREAS SHALL BE REPAIRED BY FRP OVERLAY WITH ADEQUATE LAP LENGTHS.

7.0 Load Test

7.1 Overview

Load testing of a bridge structure can be performed for any of the following reasons:

- For a new bridge, a load test can be used to verify the structural performance predicted during design. It can also provide a benchmark for comparison with future load tests to monitor the effects of time-dependent changes in the bridge properties.
- For an existing bridge, a load test can determine the load rating for the bridge more accurately than an analytical study of the bridge structure. This is particularly important when the bridge is older and has experienced damage or deterioration, which are difficult to model accurately in an analytical evaluation.
- Finally, a load test can be used to evaluate the improvement produced by repair or retrofit of a bridge structure. By performing two identical load tests before and after the repair or retrofit, the impact of the work on the bridge performance can be evaluated.

It is this latter application that is appropriate for the purposes of this report. In order to evaluate the contribution of a retrofit applied to a bridge structure, a load test performed prior to the retrofit can be repeated after the work is completed. The load test should be designed with the particular retrofit in mind so that the effects of the retrofit have as big an effect as possible on the load test results.

7.2 Load Test Parameters

It is important that a load test used to evaluate the performance of a retrofit be designed to monitor the changes in the bridge behavior that will be affected by the retrofit. This affects both the way in which the load test is performed, as well as the instrumentation used to monitor the structural performance. For example, a retrofit intended to stiffen a bridge girder would be best evaluated through monitoring of vertical deflections of the girder under load. On the other hand, a retrofit applied to increase the flexural capacity of a girder would be better evaluated through monitoring stresses in the

girder material rather than deflection monitoring. It is also important to select a loading level and layout that best evaluate the retrofit performance.

It is seldom financially viable to monitor every possible effect on the bridge structure, so it is important to determine those effects most likely to validate the performance of the retrofit. In addition, time and financial restraints will limit the number of loading levels and load patterns that can be considered during the load test. The most appropriate loading sequence must be determined prior to the load test.

7.3 Analytical Modeling

It is essential for the proper design of a load test to perform a detailed analytical study of the structure when subjected to various load levels and load patterns. The analytical model created for the design of the retrofit can be used for this purpose. Various load levels and patterns should be considered to determine which produces the best evaluation of the retrofit without jeopardizing the bridge performance. For load rating evaluation, it is necessary to subject the bridge to loads close to or even in excess of the service loading condition. However, evaluation of the effects of a retrofit should be possible with loading levels less than the service load condition. This reduces the potential for damage to the structure during the load test.

Since the test will be performed both prior to and after the retrofit, the load level should be determined based on an evaluation of both test conditions. Clearly the load test should be at a level that will not cause additional damage to the existing structure prior to the retrofit. In addition, when the same load test is applied to the retrofitted structure, sufficient variation in performance must result so that the retrofit can be evaluated.

Analytical prediction of the bridge performance during the load test provides a useful guide for the design and placement of the load test instrumentation. Based on the results of a preliminary analytical study, instrumentation can be selected and placed in the most appropriate locations to monitor the desired performance variables. This will help to reduce the number of instruments required, without jeopardizing the results of the load test.

The analytical study also provides a benchmark against which the load test results can be evaluated. It is likely that assumptions made during the analytical study may have to

be adjusted based on the results of the load test. Material properties, particularly of embedded elements such as reinforcement and prestressing steel, are hard to determine accurately without destructive testing. The assumed properties can be modified based on the results of the load test performed prior to the retrofit. This will allow for a more accurate evaluation of the net effect of the retrofit on the bridge performance.

The analytical model will likely be the same model that was used to design the retrofit. It should be detailed enough to model parameters that may affect the bridge performance. Field determined dimensions, member section properties, material properties, and support conditions should be modeled as accurately as possible. Accurate field measurements should be used to augment the dimensions shown on the construction documents. Coring of concrete in non-critical regions will provide an estimate of the compressive strength, modulus of elasticity and Poisson's ratio for use in the analytical model. The location and quantity of reinforcement and prestressing steel will have to be based on what is shown in the construction documents. However, non-destructive testing can be used to confirm reinforcement location, spacing and possibly size of bars.

Parametric studies should be performed using the analytical model to determine the effect of variations in each of the important input variables. Subsequent to the load test on the original structure, the model parameters may need to be modified to produce a closer correlation between the analytical prediction and the observed behavior. Having an understanding of the effects of variations in different parameters will simplify this correlation effort.

7.4 Instrumentation

7.4.1 General

During a load test, it is important that adequate measurements be taken to evaluate the structural performance of the bridge. The instrumentation system must be designed to suit the structural system of the bridge being tested and must be specifically designed for the loading to be applied. There is no generic instrumentation system that can be applied to all load tests. The following sections are intended to assist in the design of a suitable instrumentation system.

7.4.2 Types of Instrumentation

The most common measurements required during a load test are material strains and member deformations. Strain measurements are generally performed using one or more types of strain gage while member deformations can be monitored using displacement transducers, taut-wire deflection systems, optical surveys or GPS deflection monitors. Ambient weather conditions should also be monitored during the load test. The various types of instrumentation are described briefly in this section along with some of the advantages and disadvantages of each type of instrument. More detailed descriptions of the various instruments are given in Appendix A.

7.4.3 Strain Measurements

Vibrating Wire Strain Gages: Vibrating Wire Strain Gages (VWSG) are based on monitoring the natural frequency of vibration of a high-tension wire spanning between two end plates. As the end plates move relative to each other, the tension in the wire changes. The resulting change in the natural frequency of vibration of the wire can be correlated to the change in length of the strain gage. These gages are available from a number of suppliers and are designed for attachment to the outside of steel or concrete members, or for direct embedment in concrete.

Vibrating wire strain gages have excellent long-term zero stability and automatic monitoring of both compressive and tensile strains. The advantage of the vibrating wire strain gages over more conventional electrical resistance gages lies mainly in the use of a frequency measurement, rather than a resistance, as the output signal from the gage. Changes in lead wire length and resistance at lead connections do not affect the frequency of the vibrating wire, and therefore do not impact the reading. Vibrating wire strain gages that are attached to the surface of steel or concrete members can be reused after each load test. This helps to offset the higher unit cost of these gages compared with more conventional electrical resistance gages, which are not reusable. See Appendix A for more detailed information on vibrating wire strain gages.

Electrical Resistance Strain Gages: Electrical resistance strain gages (ERSG) usually consist of a polyimide-encapsulated constantan foil grid attached to a flexible backing

material. The gages are bonded to the surface of steel or concrete members to measure the average strain over the length of the gage. The strain reading is derived from a measurement of the change of resistance of the strain gage as the foil grid is extended or compressed along with the underlying material. In order to obtain consistent readings that accurately represent the strain in the member, the gage must be properly attached to the surface and the resistance of the lead wires and connections must not vary during the test. Any variation in lead wire resistance will affect the zero reading taken at the start of the load test. See Appendix A for more detailed information on electrical resistance strain gages.

Fiber Optic Strain Gages: Fiber optic technology is finding increasing application in sensor development. A number of fiber optic strain gages are commercially available. Although their utilization in field instrumentation projects is in its infancy, laboratory testing has verified that fiber optic sensors (FOS) are capable of measuring strain, temperature, pressure, acceleration and other variables (Measures, 2001).

These sensors have significant advantages over more traditional electrical-based sensors. They are extremely small in diameter, very light, sensitive to strain and temperature changes, resistant to corrosion and fatigue, immune to electrical interference, and do not represent electrical pathways within a host structure. No protection is required against lightning and various forms of electromagnetic interference. Even though the individual fibers on which the sensor is based are fairly fragile, once packaged for field application, commercial FOS are as robust as traditional electrical sensors (Measures, 2001). See Appendix A for more detailed information on fiber optic strain gages.

7.4.4 Deflection Measurements

An overall deflected shape of the bridge spans provides vital insight into the structural performance during the load test. This deflected shape can also be compared with the analytical results to verify bridge performance. A number of systems are available for deflection monitoring.

Optical Survey: An optical survey of the roadway surface is the simplest means for obtaining the deflected shape. An initial survey performed prior to placing load on the bridge is compared with subsequent surveys under load to produce a deflected shape.

Survey points should be determined ahead of the load test and logistics of personnel and equipment organized well in advance. Elevation readings can be taken at numerous points along each span, but should include at least the support, quarter span and midspan, at both sides of the deck and along the centerline of the roadway. The actual monitoring points should be predetermined and well marked for easy identification during the load test. A pneumatic or powder driven pin can provide an ideal survey point on most surfaces. If loading is applied using trucks, it will be necessary for the surveyors to work around the trucks to reach all monitoring points.

Optical surveys are time-consuming and have a limited accuracy. However, they can provide a reliable backup to verify any measurements determined by other means.

Direct Deflection Measurement: If logistically possible, direct deflection measurements can be made from the ground to the bridge structure. This is most commonly used for overpasses where access below the bridge is easy, but may also be possible in other locations. Displacement transducers can be attached to the soffit of the bridge with spring-loaded lines to the ground below. Relative movement between the bridge and the ground will then represent deflection of the bridge under load. Care should be taken not to locate ground-based sensors close to the pier or abutment foundations as movement of the substructure under load may affect the ground surface adjacent to the foundations.

Base-line system: A base-line system, consisting of a constant tension piano wire strung between piers, can also be used for monitoring bridge span deflections (Lee, 1995). This system is based on a reference line provided by a taut piano wire, and measurements between this reference and the bridge girders or deck. A detailed description of this system is included in Appendix A.

Tiltmeters: Tiltmeters can be located along the bridge span to measure girder rotation. The deformed shape can then be determined from the slopes at each tiltmeter location. In combination with span deflection measurements, these rotations can provide a complete deflected shape for the bridge spans being loaded. See Appendix A for more detailed information on Tiltmeters.

Deflected shape through strain measurements:

The bridge deflected shape can also be determined from strain gages located on the top and bottom surfaces of the bridge. These strain readings taken at various locations along the bridge are used to generate the bridge curvature. By curve-fitting a suitable polynomial through these discrete curvature values, an approximate expression is obtained for the bridge curvature. Double integration of this polynomial expression results in the deformed shape of the bridge. The constants of integration are solved using the known end conditions at the bridge piers or supports. This procedure is described in more detail by Vurpillot et al. (1998) and Fung et al. (2002).

GPS Deflection Monitors:

The Global Positioning System (GPS) has been used effectively for many applications, including precision land surveying. By means of a reference GPS sensor located over a known point, the position of a roving sensor can be corrected to within millimeters of its exact location. This same principle can be applied to deflection monitoring of structures. A reference GPS sensor is located over a known benchmark away from the bridge structure. GPS sensors are placed at locations on the bridge where deflection measurements are required. By correcting their location with respect to the known reference sensor, these local sensors will provide accurate three-dimensional location of their position during loading.

Video Capture:

Deformation of an object under load can be determined from analysis of high-resolution camera images taken during loading. By locating a high-resolution digital video camera adjacent to the bridge structure during the load test, computer analysis of successive digital images can be used to determine the deflection of the bridge under load.

7.4.5 Ambient Weather Conditions

Ambient weather conditions may affect data collected during a load test. It is important to record weather conditions at the site throughout the load test. The most

significant effect will generally result from changes in the ambient temperature and the surface temperature of the bridge. Ideally the load test should be performed early in the morning when the air temperature is relatively constant and solar radiation does not affect the surface temperature of the bridge. If this is not possible, or if the load test extends beyond mid-morning, it may be necessary to adjust instrument readings and measured deflections for thermal effects. The top surface of a bridge warms considerable due to daily solar radiation, while the temperature of the rest of the bridge remains relatively constant. This will result in temperature-induced strains in the top surface and consequent deformations of the bridge. These deformations are difficult to estimate without the use of a detailed computer model of the bridge structure (Ao and Robertson, 1999).

7.4.6 Data Collection

Ideally, all data collection should be automated by means of data loggers. This provides rapid, reliable data collection during the load test. If manual readings are required for certain instruments, two individuals familiar with the instrument operation should collect two independent sets of data. If any two independent readings do not agree, new readings should be taken until agreement is reached. Once the load test is completed it is too late to discover errors in the data.

Reference or zero readings must be taken on all instruments immediately prior to the application of load. It is crucial that these initial readings are accurate since all subsequent readings will be compared with the initial values to determine the change induced by the applied load. Final reference readings should be taken once all load has been removed from the bridge at the end of the load test. When compared with the initial readings, these final readings will show whether there has been any permanent deformation or thermal effect during the test. If there is a significant thermal variation during the load test, it may be necessary to adjust instrument readings to compensate for these effects. Reference temperature measurements can be made using thermocouples or hand-held surface temperature sensors.

7.5 Load Application

The load to be applied to the bridge will depend on the type of load test being planned. A proof-load test will require larger loads than a verification or evaluation load

test. Generally the load is applied by means of weighted trucks positioned appropriately on the bridge roadway (Figure 7-1). The trucks can be loaded with concrete or steel weights, or with sand or gravel. Both trucks and materials can generally be rented from a local trucking company and aggregate supplier, or obtained on loan from the state or county entity performing the load test.



Figure 7-1: Load-test on the North Halawa Valley Viaduct

Once filled, the trucks must be weighed on a calibrated load-bridge immediately before delivery to the bridge site for the load test. To model the truck load correctly on the bridge, the load on each axle must be recorded separately. This can be achieved by moving the truck onto the scale one axle at a time to determine the load on each axle. To double-check these loads, the same procedure can be applied as the truck is moved off the other end of the load-bridge. If the truck cargo is gravel or sand, it must be protected from wind or rain which might alter the weight before or during the load test.

The exact dimensions of the truck wheel spacing must be measured so as to model the load application correctly in the analytical study. If multiple trucks are used, the individual wheel locations must be determined for each truck. It is also important to record the exact location of each truck during the load test so as to model the loading accurately in the computer analysis.

It is unlikely that all of the trucks will have exactly the same total weight, though it would be advisable to attempt to equalize the weights by adjusting the load added to each

truck. The trucks should be numbered, recorded separately and modeled as such in the computer analysis.

The intended locations of the truck loads should be determined during the preliminary bridge analysis. These locations should be marked clearly on the bridge prior to the load test so that there is no confusion over truck locations during the test.

7.5.1 Load Test Execution

Execution of the load test can be performed on a single day or over a number of days if necessary. Enough personnel should be on hand to perform the various measurements required. Automation of the datalogging simplifies the recording process. However, optical surveys and other manual readings will generally define the time required for each set of readings. In order to reduce thermal effects, it is advisable to perform the load test early in the morning to avoid mid-afternoon higher temperatures. Records should be kept of ambient shade temperature and surface temperature of the roadway so as to adjust for temperature effects if significant. This is particularly important if the load test spans several days.

7.5.2 Evaluation of Results

Once corrected for thermal effects, the measurements taken during the load test can be compared with the analytical predictions obtained from the prior computer analysis. Discrepancies between predicted and measured results may be the result of a number of factors including the following:

- Any variation in the modulus of elasticity of the concrete, E_c , can have a significant effect on bridge deflections and the comparison between measured strain and computed stress.
- Differences in section properties as modeled and in real life will affect deflection measurements.
- The effect of reinforcing and prestressing steel, which may not have been included in the section properties used in the analytical model.
- The stiffening effect of non-structural elements such as guardrails and service conduits connected to the bridge.

- Stiffness at expansion joints and roller supports which may have been modeled as perfect pins or rollers in the analytical model.
- Abutment or pier foundation movement which may have been ignored in the analytical model.

Changes in bridge response between two load tests performed before and after the retrofit can be very helpful in evaluating the effect of the retrofit on bridge performance (Alkhrdaji 2002).

8.0 Summary

Fiber reinforced polymers, which consist of fibers in a polymeric matrix, are an attractive material for use in strengthening structurally deficient concrete bridges. The materials are lightweight, with a high strength to weight ratio. Typical FRP systems for bridge strengthening include: wet lay-up systems, where dry, flexible fiber sheets are saturated on-site and bonded to the concrete; prepreg systems, where fiber sheets are impregnated with resin off-site but cured on-site; and precured systems, where, e.g., pultrusion plates are manufactured offsite and bonded to the concrete. This last system is directly analogous to the strengthening system that involves attaching a steel plate to the concrete structure to increase, for example, bending capacity. Advantages of FRP over the steel plate system include: 1) FRP systems are much lighter and easier to work with, making installation typically faster and easier; and 2) FRP systems are much more resistant to corrosion.

As used for strengthening of concrete bridges, FRP systems are primarily good at resisting tensile forces. Therefore, they are used much as steel reinforcement; i.e., they are used to supplement the tensile reinforcement to increase the bending capacity and they are used to supplement the steel stirrups to increase the shear capacity. (They are also used to ‘wrap’ columns, thereby confining the concrete and increasing the column capacity. However, this application is better established, and therefore it was not considered herein.)

To increase the bending capacity, FRP strips are bonded to the exterior of the tension side of the member and run longitudinally along the length of the member. Just as with steel reinforcement, care must be taken to ensure proper ‘embedment’ lengths. Because the FRP is attached externally, debonding of the strips must be prevented. Especially at the ends, proper detailing must be observed. For shear reinforcement, sheets of FRP are bonded on the exterior of the member and run transverse to the member axis. Similar requirements regarding tie-offs of the FRP sheets must be considered as are required for steel stirrups. This typically means that the shear reinforcement must be continuous around the tension side of the member and be properly embedded in the compression

zone. Alternatively, mechanical anchors can be used to attach the ends of the FRP sheets to the concrete to prevent debonding.

To aid the designer, new design guidelines are being developed regarding FRP systems. One example is ACI 440 (ACI, 2002). The design strategy is similar to that used for steel reinforcement, although it does consider the brittle failure mode of FRP as compared to the considerable plastic deformation of steel. As such, the basic concepts and procedures should be familiar to designers. One should note, however, that these are relatively new materials, and that the design process is not as mature and based on as much experience as is that for traditional reinforced concrete. As compared to other common structural materials, FRP systems can be considered to be ‘designer’ materials, as they can be tailored to satisfy a variety of criteria by the choice of fiber and resin type and quantities. Therefore, FRP systems tend to be proprietary, and the designer typically works closely with the manufacturer in selecting a system. This will likely remain the case until designers have more experience with FRP systems and the development of the systems ‘stabilize,’ i.e., the technology matures and systems are more static.

List of References

- AASHTO (1989a). 'Guide Specification for Strength Evaluation of Existing Steel and Concrete Bridges,' American Association of State Highway and Transportation Officials, Washington, D.C.
- AASHTO (1989b). 'Guide Specifications for Fatigue Evaluation of Existing Steel and Concrete Bridges,' American Association of State Highway and Transportation Officials, Washington, D.C.
- AASHTO (2000). *Manual for Condition Evaluation of Bridges..* American Association of State Highway and Transportation Officials, Second Ed., Washington, D.C.
- ACI (1998). 'Use of Epoxy Compounds with Concrete.' ACI 503R-93 (Re-approved 1998), American Concrete Institute, Farmington Hills, MI.
- ACI (2001). 'Concrete Repair Guide.' ACI 546R-96 (Re-approved 2001), American Concrete Institute, Farmington Hills, MI.
- ACI (2002). 'Guide for the Design and Construction of Externally Bonded FRP Systems for Strengthening Concrete Structures.' ACI 440R, American Concrete Institute, Farmington Hills, MI.
- Alkhrdaji, T. (2002). 'FRP: New Life for Bridges and Budgets.' *Structure*, February, pp. 10-13.
- Ao, W.C. and Robertson, I.N. (1999). 'Investigation of Thermal Effects and Truck Loading on the North Halawa Valley Viaduct.' Report UHM/CE/99-05, University of Hawaii at Manoa, Honolulu, 217 pp.
- ASTM (2000). 'Standard Test Method for Tensile Properties of Polymer Matrix Composite Materials.' ASTM D3039/D3039M-00, ASTM International, West Conshohocken, PA.
- ASTM (2002). 'Standard Test Method for Pull-Off Strength of Coatings Using Portable Adhesion Testers.' ASTM D4541-02, ASTM International, West Conshohocken, PA.
- Barr, E. (2001). 'Structural Repair and Reinforcement using Carbon Fiber Reinforced Polymer (CFRP).' *Structural Engineer*, July, pp. 20-23.
- CT (2001a). 'Contracts for I-5/Gilman Composite Bridge Finally Awarded.' *Composites Technology*, p. 10.
- CT (2001b). 'Cantilevered Sidewalk System a Lightweight Alternative for Bridge Retrofits.' *Composites Technology*, p. 12.
- CT (2002). 'Martin Marietta and NCC Install Initial C4I Bridge Deck.' *Composites Technology*, p. 13.
- DesJardin, M. (2001). 'Carbon Fiber Applications Abound in Infrastructure.' *High-Performance Composites*, July/August, pp. 40-44.

- FHWA (1995). *Recording and Coding Guide for the Structure Inventory and Appraisal of the Nation's Bridges*. Report No. FHWA-PD-96-001, Federal Highway Administration, U.S. Department of Transportation, Washington, D.C.
- Fung, S., Aberle, M. and Robertson, I.N. (2002). 'Bridge Deflection Measurements during Earthquake Ground-Shaking.' *Proceedings of the IABSE 2002 Symposium*, Melbourne, Australia.
- Hranac, K. C. (2001). 'Carbon/Fiberglass Bridge Deck Carries the Load.' *High-Performance Composites*, July/August, pp. 52-54.
- ICRI (1995). 'Guide for Surface Preparation for the Repair of Deteriorated Concrete Resulting from Reinforcing Steel Corrosion.' IRCI 03730, International Concrete Repair Institute, Des Plaines, IL.
- ISIS (2000). 'Strengthening Reinforced Concrete Structures with Externally-Bonded Fibre Reinforced Polymers.' ISIS-M05-00, ISIS Canada.
- Khalifa, A., Gold, W. J., Nanni, A. and Abdel Aziz, M. I. (1998). 'Contribution of Externally Bonded FRP to Shear Capacity of Flexural Members.' *Journal of Composites for Construction*, ASCE, Vol.2, No.4, pp.195-202.
- Lee, A. and Robertson, I.N. (1995). 'Implementation and Long-Term Monitoring of the North Halawa Valley Viaduct,' Report UHM/CE/95-08, University of Hawaii at Manoa, Honolulu, 149 pp.
- Lichtenstein, A.G. (1993). 'Bridge Rating Through Nondestructive Load Testing,' Technical Report, NCHRP Project 12-28(13)A, June.
- Measures, R. M. (2001). *Structural Monitoring with Fiber Optic Technology*, Academic Press, London, UK.
- Meier, U. (1992). 'Carbon Fiber-Reinforced Polymers: Modern Materials in Bridge Engineering.' *Structural Engineering International*, Vol. 2, No. 1, pp. 7-12.
- Moses, F. and Verma, D. (1987). 'Load Capacity Evaluation of Existing Bridges,' NCHRP Report 301, December.
- NCHRP (1998). 'Manual for Bridge Rating Through Load Testing,' National Cooperative Highway Research Program, Transportation Research Board, Washington, D.C.
- Strongwell (2002). 'Profile,' Quarterly Newsletter from Strongwell Corporation, Bristol, VA, Spring, pp. 1-2.
- Svaty Jr., K. J., Lane, M., Grace, N. F., and Thomas, J. (2000). 'City of Wichita Implements Pioneering Rehab Technologies.' *Concrete International*, Vol. 22, No. 11, pp. 38-42.
- Triantafillou, T. C. and Antonopoulos, C. P. (2000). 'Design of Concrete Flexural Members Strengthened in Shear with FRP.' *Journal of Composites for Construction*, ASCE, Vol.4, No.4, pp.198-205.

Udd, E., Schulz, W., Seim, J., Corones, J., Laylor, H.M. (1998) “Fiber Optic Sensors for Infrastructure Applications”, Report #FHWA-OR-RD-98-18, Oregon Department of Transportation.

Vurpillot, S., Krueger, G., Benouaich, D., Clement, D., and Inaudi, D. (1998). ‘Vertical Deflection of a Pre-Stressed Concrete Bridge Obtained Using Deformation Sensors and Inclinometer Measurements.’ *ACI Structural Journal*, Vol.95, No.5, pp. 518-526.

Appendix A

A.1 Strain Measurements

Vibrating Wire Strain Gages: Vibrating Wire Strain Gages (VWSG) are based on monitoring the natural frequency of vibration of a high-tension wire spanning between two end plates. As the end plates move relative to each other, the tension in the wire changes. The resulting change in the natural frequency of vibration of the wire can be correlated to the change in length of the strain gage. These gages are available from a number of suppliers and are designed for attachment to the outside of steel or concrete members, or for direct embedment in concrete. Figure A-1 shows a Geokon model VCE-4200 embedment gage with a 6 inch gage length. VWSGs are available in gage lengths from 4 inches up. This allows for automatic averaging of strains over the gage length, an important consideration for concrete strain measurements to avoid localized strain fluctuations due to cracking or the presence of aggregate below the concrete surface.

Vibrating wire strain gages have excellent long-term zero stability and automatic monitoring of both compressive and tensile strains. The advantage of the vibrating wire strain gages over more conventional electrical resistance gages lies mainly in the use of a frequency measurement, rather than a resistance, as the output signal from the gage. Changes in lead wire length and resistance at lead connections do not affect the frequency of the vibrating wire, and therefore do not impact the reading.

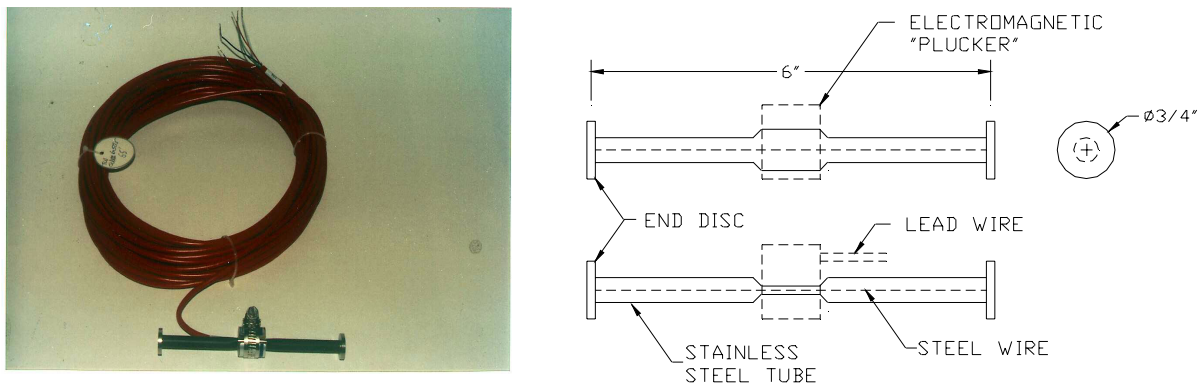


Figure A-1: Geokon VCE-4200 vibrating wire strain gage designed for concrete

Vibrating wire strain gages are known to display very stable readings during long-term field conditions. The short duration of a bridge evaluation load test would not necessarily benefit from this factor, however, if the load test were to be repeated in the future, it would be possible to leave the gages in place until the future test. Any changes in strain between load tests could be monitored accurately.

It is important to estimate the maximum strain anticipated during the load test so as to order a gage with adequate strain range. If the capacity of the gage is exceeded, either in tension or compression, the vibrating wire response becomes non-linear and is no longer reliable. It should also be noted that these gages only provide reliable readings once the end plates are firmly attached to the steel or concrete surface or embedded in the concrete. Prior to stabilizing the end plates, the readings will fluctuate. Zero readings must therefore be taken after attachment of the end plates or after first setting of the concrete for embedded gages.

Vibrating wire strain gages that are attached to the surface of steel or concrete members can be reused after each load test. This helps to offset the higher unit cost of these gages compared with more conventional electrical resistance gages, which are not reusable. The gages can be monitored using a portable readout box (Figure A-2a) or a multi-channel automated datalogger (Figure A-2b). The choice of readout instrument will depend on the number of gages to be monitored and the available budget. Both types of readout instrument can be reused on future VWSG monitoring projects.

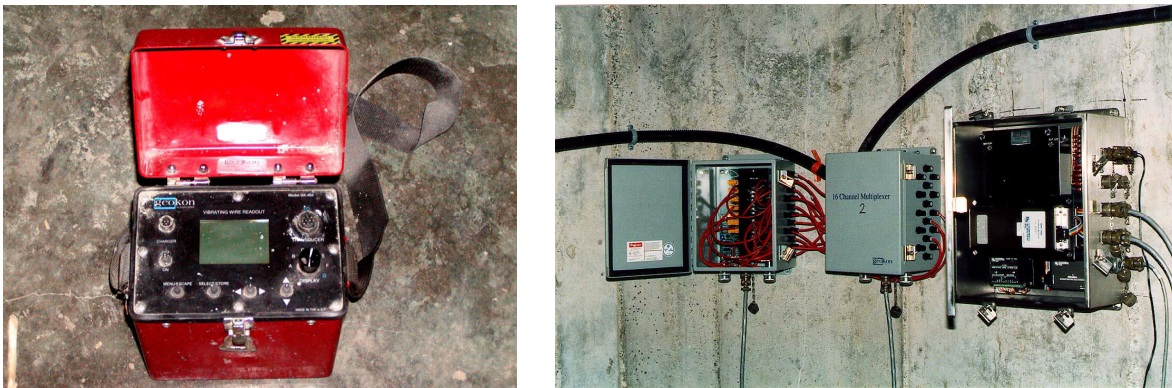


Figure A-2: a) VWSG manual readout box and b) automated datalogger

Electrical Resistance Strain Gages: Electrical resistance strain gages (ERSG) usually consist of a polyimide-encapsulated constantan foil grid attached to a flexible backing material. The gages are bonded to the surface of steel or concrete members to measure the average strain over the length of the gage. The strain reading is derived from a measurement of the change of resistance of the strain gage as the foil grid is extended or compressed along with the underlying material. In order to obtain consistent readings that accurately represent the strain in the member, the gage must be properly attached to the surface and the resistance of the lead wires and connections must not vary during the test.

Attachment of the strain gage is performed using epoxy (for steel or concrete) or spot welding (for steel applications). The strain gage manufacturer's instructions must be followed carefully to ensure proper bond between the gage and the material surface. Attachment of the lead wires to the gage terminal tabs may lead to damage of the sensitive gage foil or the epoxy bond. It is recommended that gages be ordered with short lead wires already attached. Additional lead wire length can then be added in the field without potential for damaging the gage. Figure A-3 shows an ERSG attached to steel reinforcement by means of epoxy. The gage is subsequently covered with wax and electrical tape to protect it during embedment in the concrete. Figure A-4 shows an ERSG welded to the surface of a steel section. This spot-welding procedure is often easier than the epoxy application, though the initial cost of the strain gages is higher. Figure A-4 shows an ERSG applied to the surface of a concrete beam using epoxy. In this application the gage length should be at least twice the aggregate size to allow for strain averaging over a representative section of concrete.

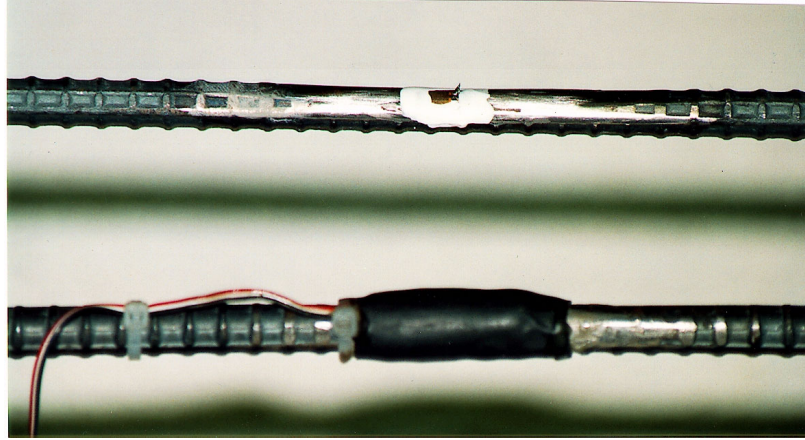


Figure A-3: Electrical resistance gages epoxy bonded to steel reinforcement

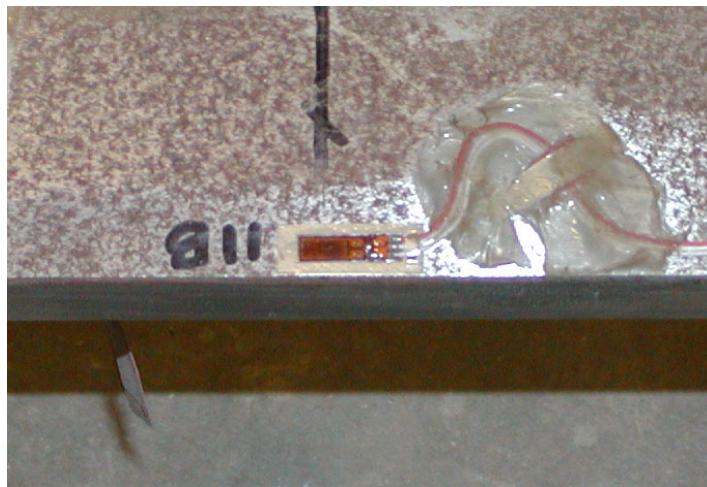


Figure A-4: Electrical resistance gage spot-welded to steel section

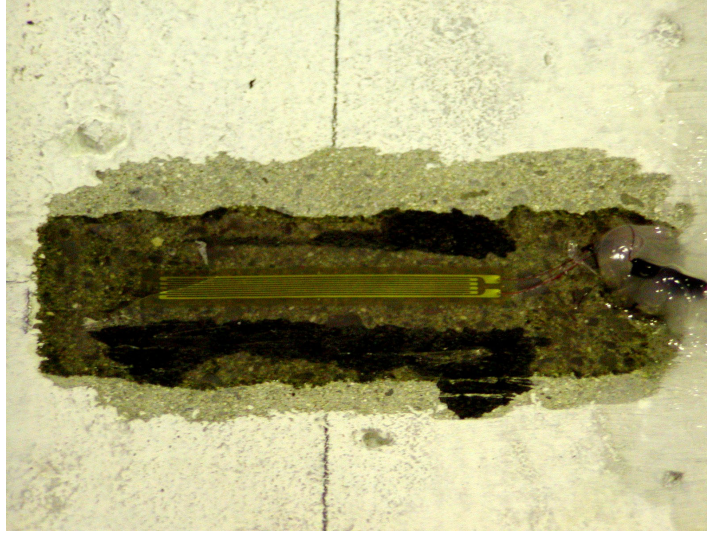


Figure A-5: Electrical resistance gage epoxy bonded to surface of concrete

Any variation in lead wire resistance will affect the zero reading taken at the start of the load test. It is therefore important that the lead wires remain connected to the readout box throughout the load test. If it is necessary for the strain gage leads to be disconnected from the datalogger it is essential that readings be taken immediately prior to and after the reconnection of the lead wires. Even so, there will be some doubt about the change in readings resulting from the changed resistance at the connector. Compensation for temperature changes of the lead wire is standard for most strain gage readout equipment through the use of a return loop that does not pass through the strain gage. The lead wire must have three strands for this compensation to function correctly.

In order to protect strain gages from moisture, they are generally encapsulated with a waterproof coating after attachment to the member surface. This is also necessary to protect the epoxy bond, which may not be waterproof, and to protect the gage from incidental impact during the test.

Strain gages can be used for flexural strain monitoring of steel or concrete flexural members, axial strain monitoring of columns or shear strain monitoring using an array of strain gages located on the web of the member.

Long gage lengths are available for use on concrete members where average strains over a gage length of 2 or more inches are more reliable than strains measured over

shorter gage lengths which may be affected by localized cracking or the presence of aggregate below the strain gage location.

Fiber Optic Strain Gages: Fiber optic technology is finding increasing application in sensor development. A number of fiber optic strain gages are commercially available. Although their utilization in field instrumentation projects is in its infancy, laboratory testing has verified that fiber optic sensors (FOS) are capable of measuring strain, temperature, pressure, acceleration and other variables (Measures, 2001).

These sensors have significant advantages over more traditional electrical-based sensors. They are extremely small in diameter, very light, sensitive to strain and temperature changes, resistant to corrosion and fatigue, immune to electrical interference, and do not represent electrical pathways within a host structure. No protection is required against lightning and various forms of electromagnetic interference. Even though the individual fibers on which the sensor is based are fairly fragile, once packaged for field application, commercial FOS are as robust as traditional electrical sensors (Measures, 2001) (Figure A-6).

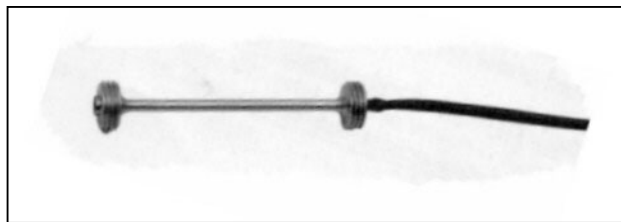


Figure A-6: Fiber optic strain sensor for concrete embedment

FOS technology is based a number of different principles involving the passage of light through an optical fiber. Three of the most common sensor systems are described briefly below.

Micro-bending:

Generally an optical fiber consists of a small diameter glass core surrounded by a thicker coating with a lower index of refraction. Light input at one end of the core is “trapped” in the core by reflection at the interface between the core and coating. If the fiber is bent around a sharp angle, however, this internal reflection will decrease, and some of the light signal will be lost into the coating. The remaining signal at the other end of the glass core will be reduced. This is the principle behind micro-bending sensors as

illustrated in Figure A-7. Pressure on the clamping mechanism will induce micro-bending which will reduce the light output. This drop in output can be correlated to the applied pressure to produce a pressure transducer. The advantage of these gages is the simplicity of operation. The light source can be a broadband (white) light and the readout is provided by a light meter.

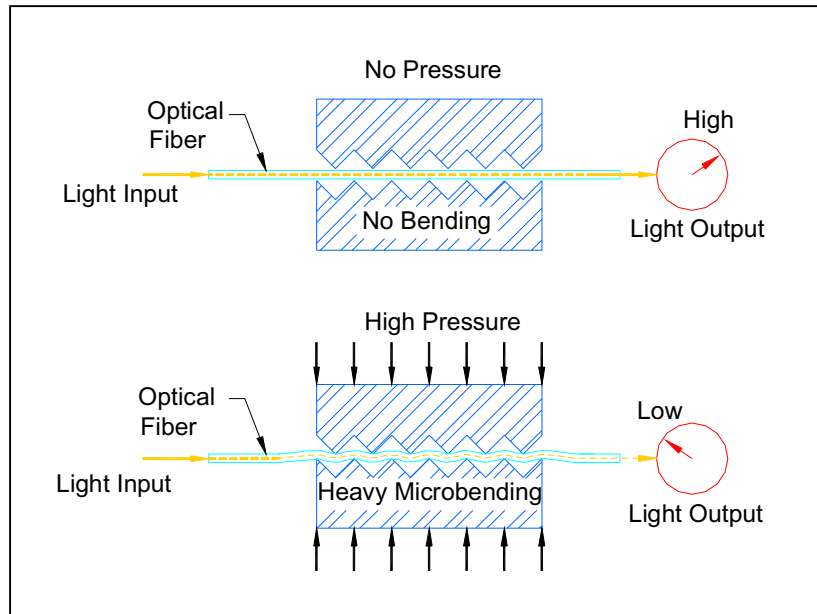


Figure A-7: Operation of microbending fiber optic sensor

Fabry-Perot Sensors: Figure A-8 shows the principle behind Fabry-Perot or gap-based fiber optic sensors. A narrow band light source is input at one end of an optical fiber with a mirrored gap at the sensor location. As the light passes through the gap, some of the input is reflected back and forth between the mirrors. This results in a series of phase shifts in the output signal. The phase shift can be correlated with the distance between the mirrored fiber ends. By attaching the mirrored fiber ends to adjacent points on the surface of a structural member, any movement between the mirrors can be correlated to strain in the member at the location of the fiber gap. Fabry-Perot sensors can also be based on a single-ended fiber with a mirrored gap at the end of the fiber as shown in Figure A-9.

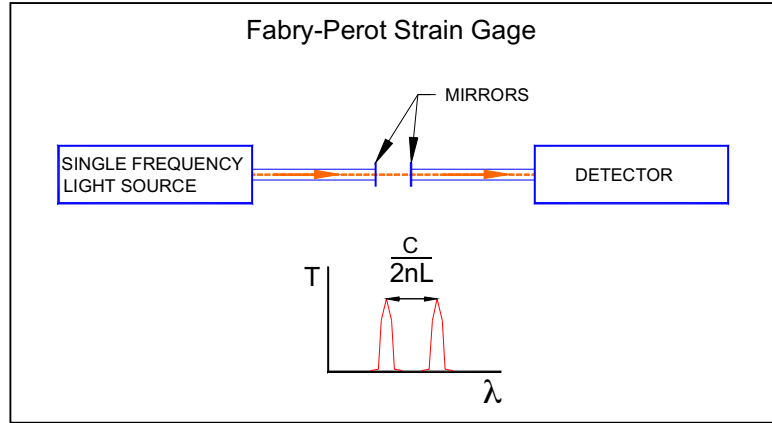


Figure A-8: Fabry-Perot in-line strain sensor

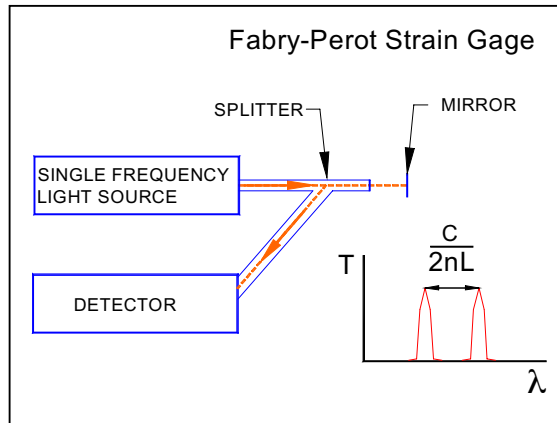


Figure A-9: Fabry-Perot terminal strain sensor

Bragg Grating Sensors: The refractive index of an optical fiber core can be changed by exposure it to an ultra-violet source. By using two interfering UV sources, it is possible to create a “grating” with a different refractive index from that of the rest of the fiber core (Udd, 1998) (Figure A-10). As broadband light passes through this Bragg Grating, light with a wavelength equal to the spacing of the grating will be reflected, while the rest of the light will pass through. Either the reflected light or output light can be analyzed to determine the frequency corresponding to the Bragg Grating. If the fiber containing the Bragg Grating is now deformed as part of a strain gage, the frequency of the reflected light will change. This frequency change can be correlated to the elongation of the Bragg Grating and so to the strain or displacement causing that elongation. By creating Bragg Gratings with different initial spacings, a single fiber can be used for multiple sensors (Figure A-11).

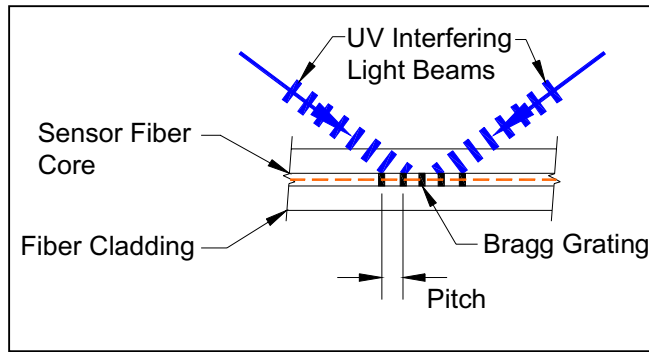


Figure A-10: Creating Bragg Grating fiber optic sensor

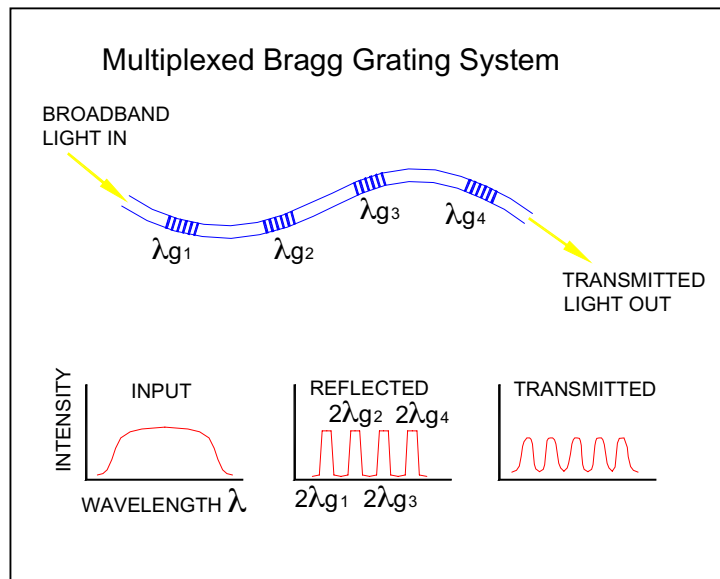


Figure A-11: Multiplexed Bragg Grating fiber optic sensors

Strain Gage Locations:

For a load test of an existing structure, the strain gages will be attached to the surface of individual structural members. The location of the gages will depend on the information required from the load test. If there is interest in the performance of the deck slab, gages would need to be placed at highly stressed locations on this slab. If there is interest in the performance of the bridge girders or piers, suitable gage locations would be selected to monitor the strains at locations anticipated to have the largest strain induced during the load test. As with all instrumentation, there is always a margin of error in the strain gage readings. It is important that the strain sensors selected for the load test are

sensitive enough to accurately monitor the anticipated strains based on the pre-test analytical study of the bridge under the load test conditions.

Measurement of strains in deck slabs will normally require placement of strain sensors at points of maximum bending moment. Sensors should be placed on both tension and compression faces (if possible) to determine the neutral axis location and allow for stress resolution at the level of the reinforcement in the slab. Because deck slabs are generally continuous over the girders, strain measurements should be made at locations of both negative and positive bending.

Bridge girders are often simply supported between bents. This is typical of precast concrete girders and steel plate girders. Strain measurements will generally be made at midspan on both top and bottom flanges of the girder. If shear stresses are of concern, a strain gage rosette can be located on the girder web in the shear span to determine principal strain magnitude and direction.

Continuous box-girder bridges that extend for two or more spans between expansion joints will require strain monitoring at both midspan and supports.

A.2 Deflection Measurements

Base-line system: A base-line system, consisting of a constant tension piano wire strung between piers, can also be used for monitoring bridge span deflections (Lee, 1995). This system is based on a reference line provided by a taut piano wire, and measurements between this reference and the bridge girders or deck. Figure A-12 illustrates this system schematically. One end of the piano wire is fixed to a pier or part of the girder at one end of the span. The other end passes over a pulley at the opposite end of the span and supports a weight equal to between 60 and 80% of the break strength of the piano wire (Figure A-13b). This arrangement assures a constant catenary for the reference baseline. Measurements are then made using a digital caliper between the baseline and fixed locations on the girder or bridge deck (Figure A-13a). Changes in these readings indicate movement of the bridge girder relative to the end supports. Replacing the manual caliper readings with Linear Variable Displacement Transducers (LVDTs) would enable automated monitoring of the deflected shape.

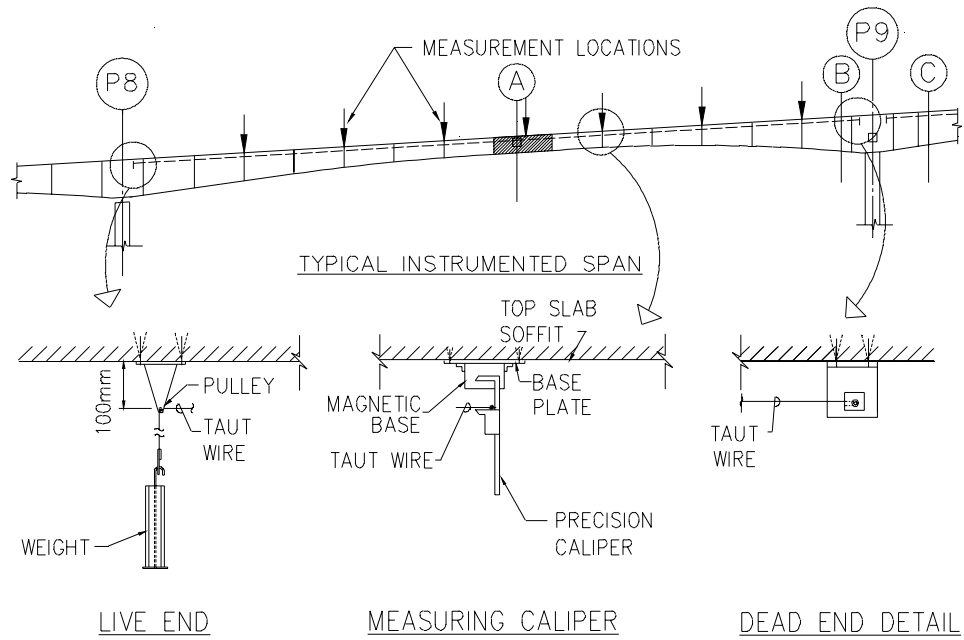


Figure A-12: Baseline deflection system using taut piano wire as reference



a) measuring digital caliper



b) constant weight reference

Figure A-13: Components of baseline system

Tiltmeters: Tiltmeters can be located along the bridge span to measure girder rotation (Figure A-14). The deformed shape can then be determined from the slopes at each tiltmeter location. In combination with span deflection measurements, these rotations can provide a complete deflected shape for the bridge spans being loaded. Since the amount of rotation is likely to be small, it is important that the tiltmeters be accurate enough to monitor the rotation anticipated at each location. Tiltmeters can be “wall” or “floor” mounted and can be removed and reused on future projects. Readings can be taken using a handheld readout or an automated datalogger.

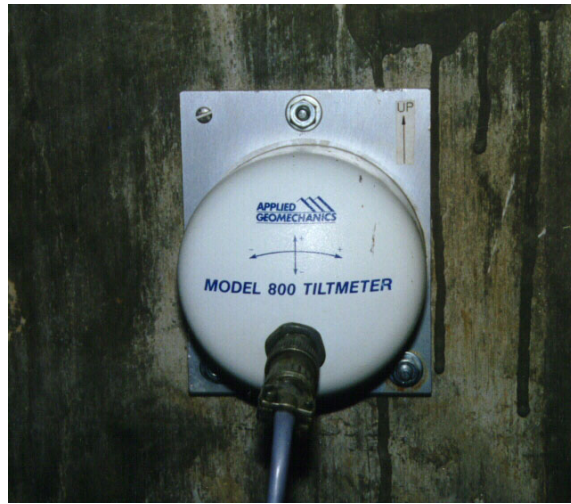


Figure A-14: Tiltmeter attached to concrete girder web